AD-A082 435 BELFER GRADUATE SCHOOL OF SCIENCE NEW YORK F/G 20/3
SYSTEMATIC STUDY OF PYROELECTRICITY. APPLICATIONS OF PYROELECTR--ETC(U)
JUL 79 M I BELL, Y H TSUO DAAB07-76-C-1342
UNCLASSIFIED DELET-TR-76-1342-F NL

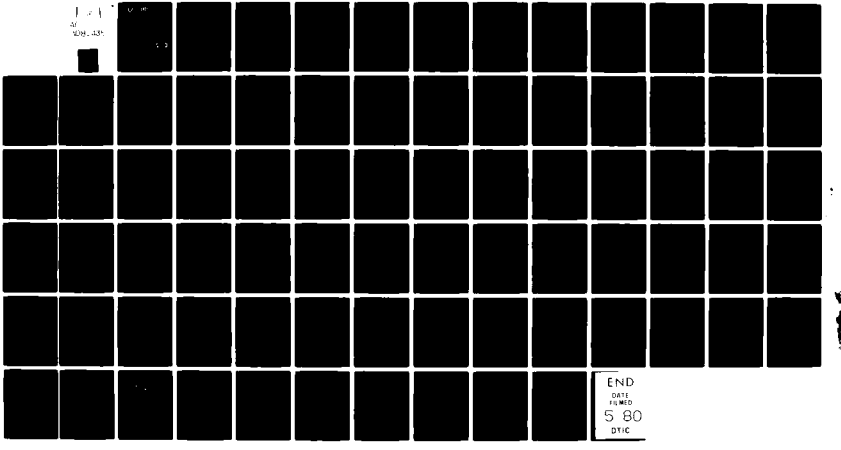

END
DATE FILMED
5 80
DTIC

LEVEL II

RESEARCH AND DEVELOPMENT TECHNICAL REPORT

DELET-TR-76-1342-F

AD A082435

SYSTEMATIC STUDY OF PYROELECTRICITY

APPLICATIONS OF PYROELECTRIC MATERIALS

M. I. Bell and Y. H. Tsuo
Yeshiva University
Belfer Graduate School of Science
2495 Amsterdam Avenue
New York, New York 10033

July 1979

Final Report for Period 1 October 1975 - 31 March 1977

SPONSORED BY.

DEFENSE ADVANCED RESEARCH PROJECTS AGENCY
1400 WILSON BLVD.
ARLINGTON, VA. 22209
ARPA ORDER NO. 2573

ERADCOM

US ARMY ELECTRONICS RESEARCH & DEVELOPMENT COMMAND
FORT MONMOUTH, NEW JERSEY 07703

NOTICES

Disclaimers

The citation of trade names and names of manufacturers in this report is not to be construed as official Government indorsement or approval of commercial products or services referenced herein.

Disposition

Destroy this report when it is no longer needed. Do not return it to the originator.

UNCLASSIFIED

SECURITY CLASSIFICATION OF THIS PAGE (When Data Entered)

REPORT DOCUMENTATION PAGE

READ INSTRUCTIONS BEFORE COMPLETING FORM

1. REPORT NUMBER: DELET TR-76-1342-F	2. GOVT ACCESSION NO.
3. RECIPIENT'S CATALOG NUMBER	
4. TITLE (and Subtitle): Systematic Study of Pyroelectricity and Applications of Pyroelectric Materials	5. TYPE OF REPORT & PERIOD COVERED: Final Technical Report. 1 Oct 1975 — 31 Mar 1977
6. PERFORMING ORG. REPORT NUMBER	
7. AUTHOR(s): M.I. Bell and Y.H. Tsuo	8. CONTRACT OR GRANT NUMBER(s): DAAB07-76-C-1342
9. PERFORMING ORGANIZATION NAME AND ADDRESS: Yeshiva University, Belfer Graduate School of Science, 2495 Amsterdam Ave., New York, NY 10033	10. PROGRAM ELEMENT, PROJECT, TASK AREA & WORK UNIT NUMBERS: Program Code No. 2573
11. CONTROLLING OFFICE NAME AND ADDRESS: Advanced Research Projects Agency, 1400 Wilson Blvd., Arlington, VA 22209	12. REPORT DATE: Jul 1979 13. NUMBER OF PAGES: 77
14. MONITORING AGENCY NAME & ADDRESS (if different from Controlling Office): US Army Electronics Command, Fort Monmouth, NJ 07703 DRSEL-TL-ES	15. SECURITY CLASS. (of this report): Unclassified 15a. DECLASSIFICATION/DOWNGRADING SCHEDULE

16. DISTRIBUTION STATEMENT (of this Report)

Approved for public release; distribution unlimited

17. DISTRIBUTION STATEMENT (of the abstract entered in Block 20, if different from Report)

18. SUPPLEMENTARY NOTES: This research was supported by Advanced Research Projects Agency of the Department of Defense and was monitored by US Army Electronics Command under Contract No. DAAB-07-76-C-1342. ARPA Contractor; Yeshiva U, M.I. Bell, Principal Investigator, (212)-568-8400. Project Scientists: F.Rothwarf, (210)-544-4407; G.J. Iafrate, (201)-544-4070).

19. KEY WORDS (Continue on reverse side if necessary and identify by block number)

Ferroelectrics, Pyroelectric detectors, Figure of merit, Phase transitions, Molecular field theory, Triglycine sulfate, Postassium niobate, Raman scattering, Vidicons.

20. ABSTRACT (Continue on reverse side if necessary and identify by block number)

Full accounts are given of theoretical and experimental studies of ferroelectric phase transitions begun under a previous contract and completed under the present one. present one. The findings of these studies are applied to the analysis of several applications of pyroelectric materials and to the evaluation of the suitability of various ferroelectrics for these uses. A major result is that improper ferroelectrics, in which the polarization is not the order parameter, are predicted to have performance superior to that of proper ferroelectrics in both

DD FORM 1 JAN 73 1473 EDITION OF 1 NOV 65 IS OBSOLETE

SECURITY CLASSIFICATION OF THIS PAGE (When Data Entered)

20 Abstract (cont'd)

infrared imaging and thermal-to-electrical energy conversion applications. Experimental evidence is presented supporting this conclusion in the case of the pyroelectric vidicon.

TABLE OF CONTENTS

I. INTRODUCTION

The work described in this report was conducted between 1 October 1975 and 31 March 1977 under Defense Advanced Research Projects Agency contract DAAB 07-76-C-1342, M.I. Bell, principal investigator, F. Rothwarf, contract monitor. This investigation continued the efforts begun under a previous contract (DAAB 07-74-C-0470) to elucidate the physical mechanisms responsible for the pyroelectric effect in ferroelectrics, to discover such limitations as may exist on the performance of these materials in infrared imaging (vidicon) systems, and to obtain theoretical guidance in the search for materials which would yield improved detector performance. These objectives have been met through the development[1-3] of a generalized molecular field theory of ferroelectricity (GMFT) which has provided new insight into the nature of ferroelectric phase transitions and has led to a better understanding of the observed limitations on the performance of the materials currently used as vidicon targets[4]. A brief account of the basic elements of this theory has been prepared for publication and is contained in Section II of this report.

An underlying assumption of the GMFT is the existence of elementary dipoles which persist (although in a disordered state) at temperatures well above that of the ferroelectric-to-paraelectric transition, even in so-called displacement-type ferroelectrics. In order to determine whether effects attributable to the presence of such dipoles could be observed in the Raman scattering spectra of displacement-type ferroelectrics, a study of $KNbO_3$ was begun in collaboration with A.M. Quittet and M. Lambert[5] and completed with the help of M. Krauzman. The results of these experiments, which provide excellent support for the assumptions on which the GMFT is

based, were presented in a previous report,[6] and a revised version of that manuscript has since been published in the Physical Review[7]. A reprint of this work is provided in Appendix A.

Further experimental verification of the GMFT has been obtained from measurements of the electric field and temperature dependence of the dielectric constants of several ferroelectrics. From these measurements one can obtain the temperature dependence of the coefficients which appear in the Devonshire expansion of the free energy[8]. The GMFT predicts[1,2] that these coefficients should depend linearly on temperature, and our experimental results, presented in Section III of this report, confirm this prediction. An account of these experiments will be presented at the March 1978 meeting of the American Physical Society, and an abstract of that talk is provided in Appendix B.

Our assessment, based on the GMFT, of the potential performance of ferroelectrics as vidicon targets[4] led us to conclude that materials significantly better than those now in use are not likely to be found within the well-known families of ferroelectrics (e.g. perovskites or triglycine sulfate derivatives) or by minor modifications of these materials. We therefore turned our attention to situations in which the arguments of the GMFT would not apply and one might hope to avoid the limitations imposed by the theory. One such case is that of the improper ferroelectrics[9] (e.g. the rare-earth molybdates), where an analysis based on phenomenological models for the free energy shows that the performance of such a material as a vidicon target depends on temperature in a significantly different way than the performance of

a proper ferroelectric. The calculated performance (signal-to-noise ratio) of a proper ferroelectric target decreases rapidly as the Curie temperature is approached, but when an improper ferroelectric is used the performance is expected to approach a maximum at the Curie temperature. These results were presented to a meeting of the Materials Research Council of the Defense Advanced Research Projects Agency in July, 1976 (see Appendix C for an abstract of that report). Section IV of this report contains the details of these calculations together with preliminary experimental results which both demonstrate the theoretically predicted behavior and indicate that the increase in performance exhibited by an improper ferroelectric near its transition temperature can be great enough (more than a factor of 15) to make it competitive with the best of the materials now in use as vidicon targets.

Finally, Section V examines several potential applications of pyroelectrics in the areas of energy conversion and storage which, while not strictly within the scope of the present investigation, are of considerable current interest and depend for their success on the development of materials having many of the same properties as are required in thermal imaging systems. For each application a figure of merit is developed which permits an assessment of the relative merit of the various ferroelectric materials which might be used in that application. Results from the GMFT, from the phenomenological theory, and from the experimental literature are used to evaluate and compare these figures of merit, and several promising directions are identified for future studies aimed at achieving efficient thermal to electrical energy conversion using ferroelectrics.

References

1. M.I. Bell and P.M. Raccah, Technical Report ECOM-74-0470-1, Yeshiva University (1975).
2. M.I. Bell and P.M. Raccah, Bull. Am. Phys. Soc. 20, 359 (1975).
3. M.I. Bell and P.M. Raccah, Technical Report ECOM-74-0470-2, Yeshiva University (1975).
4. M.I. Bell and P.M. Raccah, IEDM Tech. Digest, 70 (1975).
5. A.M. Quittet, M.I. Bell, M. Cambert, and P.M. Raccah, Bull. Am. Phys. Soc. 20, 327 (1975).
6. M.I. Bell and P.M. Raccah, Technical Report ECOM-74-0470-3, Yeshiva University (1976).
7. A.M. Quittet, M.I. Bell, M. Krauzman, and P.M. Raccah, Phys. Rev. B 14, 5068 (1976).
8. A.F. Devonshire, Advan. Phys. 3, 85 (1954).
9. See, for example, A.P. Levanyuk and D.G. Sannikov, Sov. Phys. - - Usp. 17, 199 (1974).

II. GENERALIZED MOLECULAR FIELD THEORY OF FERROELECTRICITY*

by

M.I. Bell

and

P.M. Raccah+

Physics Department
Yeshiva University
New York, New York

* Research supported by the Defense Advanced Research Projects Agency

+ Present address: University of Illinois at Chicago Circle, Chicago, Illinois

The most recent and fruitful theory of ferroelectric phase transitions is based on the concept of the lattice dynamical instability, or soft mode, introduced[1] by Cochran and Anderson. Older theories employing the molecular-field approximation[2] describe the ferroelectric phase transition as an order-disorder transformation involving the ordering of an array of permanent dipoles, as in the Weiss theory of ferromagnetism. Despite a recent renewal of interest in this approach[3], it would appear not to be applicable to a large class of ferroelectrics, including the perovskites, where the structure determined for the paraelectric phase has each atom located at an inversion center, thus precluding the existence of permanent dipoles. In addition, the phase transitions predicted by the conventional molecular-field theory (MFT) are thermodynamically of second order, while many observed transitions are first order. The purpose of this communication is to show that neither of these objections should be regarded as ruling out the possibility of an adequate description of ferroelectricity based on a molecular-field theory.

With regard to the first objection, it has been pointed out[4] that the atomic sites may be inversion centers only in some average sense. For example, studies[5] of the scattering of electrons and x-rays by $BaTiO_3$ and $KNbO_3$ reveal patterns of diffuse scattering which can be interpreted[4] as arising from partially correlated displacements of the metal ions from the centers of the oxygen octahedra. The observed scattering is accounted for by assuming a relatively simple pattern of displacements resulting in the formation of chains of correlated displacements approximately 10 to 25 unit cells in length[4]. Only when averaged over distances large compared to the chain length does the crystal have the macroscopic structure determined

by x-ray diffraction. More recently, similar diffuse scattering has been seen in neutron scattering experiments[6] on $BaTiO_3$, $KTaO_3$, $KTa_xNb_{1-x}O_3$ (KTN), and $SrTiO_3$. Additional evidence for disorder in the perovskites has been obtained from Raman scattering measurements[7] and from studies of optical second-harmonic generation[8].

Although NMR measurements[9] have shown that the displacement correlations are dynamic rather than static as originally proposed[4], this is not an obstacle to the use of a molecular-field model. As noted by Yamada et al[10], the unit-cell dipole moment which appears in such calculations can be interpreted as an instantaneous value, corresponding to one of several sets of equilibrium atomic positions arranged symmetrically about the average structure. The free energy obtained by time averaging would then have the same form as if the dipoles were static.

If we take seriously the possibility that the paraelectric phases of materials which undergo ferroelectric phase transitions may be polar in the sense of containing permanent electric dipole moments, we must re-examine the order-disorder transitions predicted by the MFT. For the sake of this discussion, and without any real loss of generality, we will consider an array of N elementary dipoles of moment μ, free to assume any orientation in space, which interact via a molecular (local) field E_ℓ. The usual statistical argument then gives for the macroscopic polarization P at temperature T

$$P(T) = N\mu L(x), \qquad (1)$$

where $L(x) = \coth x - 1/x$ and $x = \mu E_\ell/kT$ (k is Boltzmann's constant). For small values of x, Eq. (1) can be solved to give the local field E_ℓ as a power series in P.

It has been customary to assume that E_ℓ has the Lorentz form

$$\vec{E}_\ell = \vec{E} + \lambda\vec{P} \tag{2}$$

where $\vec{E}$ is the applied (macroscopic) electric field, and the Lorentz factor λ has the value $4\pi/3$ for cubic or isotropic media. One can then solve for $E = \partial G/\partial P$ and obtain the free energy,

$$G = \tfrac{1}{2}A_o(T - T_o)\, P^2 + \tfrac{1}{4}B_o T\, P^4 + \frac{1}{6}\, C_o T\, P^6 + \ldots, \tag{3}$$

which has the Landau-Devonshire form[11] (i.e. a power series in the order parameter P), with

$$\begin{aligned} A_o &= 3k/N\mu^2 \\ B_o &= 3A_o/5N^2\mu^2 \\ C_o &= 99A_o/175N^4\mu^4 \end{aligned} \tag{4}$$

and

$$T_o = \lambda/A_o. \tag{5}$$

In this context, the most important fact about the free energy (3) is that B, the coefficient of the P^4 term, is positive for all finite temperatures, so that the MFT always predicts a second-order phase transition[11]. Yet, as will now show, the polar nature of the paraelectric phase offers a means of avoiding this difficulty.

It has long been known[12] that the Lorentz local field (2) is not suitable for the description of liquids composed of polar molecules. With this local field the MFT predicts a ferroelectric ordering in many common liquids at room temperature. Water, for example[12], would order at T_o = 1140 K. Among the numerous attempts to avoid this

difficulty one finds a particularly interesting and elegant approach due to Onsager[13]. He showed that in a polar medium the field which acts to align an elementary dipole with the applied field is not given by Eq. (2) but by

$$\vec{E}_\ell = \vec{E} + \frac{4\pi}{2\epsilon+1}\vec{P}. \tag{6}$$

If $\epsilon >> 1$, Eq. (6) gives $\vec{E}_\ell \simeq \vec{E} + \frac{1}{2}\chi^{-1}\vec{P}$, and since the inverse susceptibility is given by $\chi^{-1} = \partial^2 G/\partial P^2$, an expansion of the form (4) for G requires that E_ℓ contain terms involving every odd power of P:

$$E_\ell = E + \lambda_0 P + \lambda_1 P^3 + \lambda_2 P^5 + \ldots \tag{7}$$

The Onsager local field (6) takes into account only the dipole-dipole coupling and ignores any short-range interactions[14]. For this reason we treat the λ_i appearing in Eq. (7) as adjustable (temperature-independent) parameters, rather than use the specific (temperature-dependent) values predicted by the Onsager theory and given implicitly by Eq. (6). The generalized local field (7) leads to a free energy

$$G = \tfrac{1}{2}A_0(T - T_0)P^2 + \tfrac{1}{4}B_0(T - T_1)P^4 + \frac{1}{6}C_0(T - T_2)P^6 + \ldots, \tag{8}$$

where the coefficients A_0, B_0, C_0,... are given by Eq. (4), and the characteristic temperatures by

$$\begin{aligned} T_0 &= \lambda_0/A_0 \\ T_1 &= \lambda_1/B_0 \\ T_2 &= \lambda_2/C_0, \end{aligned} \tag{9}$$

and so forth. The most striking feature of this generalized molecular field theory (GMFT) is that for $T_1 > T_0$ the second Devonshire coefficient,

$$B = B_0(T - T_1), \tag{10}$$

is negative in the vicinity of T_o, and one obtains a first-order phase transition.

In comparing the predictions of Eq. (8) with experimental results, we find that in the two cases where the temperature dependence of B has been measured, the behavior predicted by Eq. (10) is actually observed. Table I lists the values of the coefficients A_o, B_o and the temperatures T_o, T_1 obtained in $BaTiO_3$[15] and triglycine sulfate (TGS)[16]. Note that in $BaTiO_3$ we find $T_1 > T_o$, as required for a first-order transition, while we have $T_1 < T_o$ in TGS where the transition is second order. This experimental data enables us to make two quantitative checks of the GMFT. First, using Eq. (4), we find for the maximum (saturation) polarization

$$N\mu = (3A_o/5B_o)^{\frac{1}{2}}, \tag{11}$$

and the data of Table I yield values of 17 and 4.9 $\mu C/cm^2$ for $BaTiO_3$ and TGS, respectively. The result for $BaTiO_3$ is somewhat smaller than the 26 $\mu C/cm^2$ found experimentally[15], but that for TGS is in excellent agreement with the experimental result[17] of 4.3 $\mu C/cm^2$. Second, Eq. (4) also gives the relation

$$N = A_o^2/5kB_o \tag{12}$$

for the number of independent dipoles per unit volume. We find densities of 1.99×10^{21} cm^{-3} and 4.6×10^{20} cm^{-3} for TGS and $BaTiO_3$, respectively. Comparing these results to the unit cell volumes, we obtain 0.8 and 33 unit cells per elementary dipole, indicating that while each unit cell in TGS

behaves as a statistically independent dipole, the effective dipoles in $BaTiO_3$ must consist of larger regions in which the polarization is highly correlated. The linear correlations proposed by Comès et al[4] to account for the diffuse x-ray scattering have a length of 10 - 25 unit cells and would satisfy this prediction of the GMFT quite well.

A major virtue of the present model is its ability to describe first order transitions, and so special attention should be paid to those quantities which are peculiar to such transitions, i.e. the difference between the Curie-Weiss temperature T_o and the actual transition temperature T_c, the discontinuity P_{sc} in spontaneous polarization, and the latent heat of the transition W. Unfortunately, accurate calculation of these quantities from the model is frustrated by a lack of experimental information concerning the coefficients λ_2, λ_3,... which determine the higher-order nonlinearities of the local field. The fact that the discontinuity in spontaneous polarization at T_c in $BaTiO_3$ is 70% of the saturation polarization[15] indicates that these nonlinearities are significant even at the transition temperature. We have found that this saturation behavior can be taken into account in an <u>ad hoc</u> but effective way by replacing the power series (7) by its lowest-order nontrivial Padé approximant,

$$E_\ell = \frac{\lambda_o P}{1-(\lambda_1/\lambda_o)P^2} . \tag{13}$$

This expression reproduces the first two terms of (7) for small P and also insures that if $\lambda_1 > 0$ the polarization will saturate, since then $P^2 < \lambda_1/\lambda_o$ for all finite values of the local field.

Using Eq. (13) for the local field, we find for the spontaneous polarization at the transisiton $P_{sc}/N\mu = 0.6$, in reasonable agreement with the experimental result cited above. We also obtain $T_c - T_o = 5K$, somewhat less than the experimental value[15] of 8K. The latent heat (integrated[18] over the interval T_o, T_c) is calculated to be 21 cal/mol, while the measured value is 47 cal/mol. Clearly, the predicted transition is not as strongly first order as that observed experimentally, but the agreement is still quite satisfactory. Further comparison of this theory with experiment and a detailed discussion of the local field (13) will be presented elsewhere.

References

1. W. Cochran, Advan. Phys. 9, 387 (1960); P.W. Anderson, in Fizika Dielekrikov, ed. by G.I. Skaravi (Ed. Acad. Nank SSR, Moscow, 1960) p. 290.
2. See, for example, W. Känzig, Solid St. Phys. 4, 1 (1957).
3. M. Lambert and R. Comes, Solid St. Comm. 7, 305 (1969); J.A. Gonzalo, Phys. Rev. B9, 3149 (1974); A.S. Chaves, F.C.S. Barreto, R.A. Nogueira, and B. Zeks, Phys. Rev. B13, 207 (1976).
4. R. Comes, M. Lambert, and A. Guinier, Solid St. Comm. 6, 715 (1968).
5. G. Honjo, S. Kodera, and N. Kitamura, J. Phys. Soc. Jpn. 19, 351 (1964); J. Horada and G. Honjo, J. Phys. Soc. Jpn. 22, 45 (1967); R. Comes, M. Lambert, and A. Guinier, Compt. Rend. 266, 959 (1968).
6. See R. Currat, R. Comes, B. Dornier, and E. Wiessendanger, J. Phys. C. 7, 2521 (1974), and refs cited therein.
7. M.P. Fontana and M. Lambert, Solid St. Comm. 10, 1 (1972); A.M. Quittet, M.I. Bell, M. Krauzman, and P.M. Raccah, Phys. Rev. B 14, 5068 (1976).
8. S.K. Kurtz, Private communication.
9. G. Bonera, F. Borsa, and A. Rigamonti, J. Phys. (Paris) 33, C2-195 (1972).
10. Y. Yamada, G. Shirane, and A. Linz, Phys. Rev. 177, 848 (1969).
11. A.F. Devonshire, Advan. Phys. 3, 85 (1954).
12. See, for example, C.P. Smyth, Dielectric Behavior and Structure (McGraw-Hill, New York, 1955) Chap. I.

13. L. Onsager, J. Am. Chem. Soc. 58, 1486 (1936).

14. H. Fröhlich, Theory of Dielectrics (Oxford, 1958).

15. M.E. Drougard, R. Landauer, and D.R. Young, Phys. Rev. 98, 1010 (1955); M.E. Drougard and E.J. Huibregtse, IBM J. Res. and Devel. 1, 318 (1957).

16. K.H. Ehses and M.E. Müser, Ferroelectrics 12, 247 (1976).

17. A.G. Chynoweth, Phys. Rev. 117, 1235 (1960).

18. See E. Fatuzzo and W.J. Merz, Ferroelectricity (J. Wiley and Sons, New York, 1967) p. 118 concerning the comparison of theory and experiment involving the latent heat.

Table I. Experimental values of parameters appearing in the free energy given by Eq. (8).

	$BaTiO_3$ (Ref. 15)	TGS (Ref. 16)
$A_o(10^{-5}$ cgs)	7.6	389
$B_o(10^{-13}$ cgs)	0.18	110
T_o(K)	378	322.4
T_1(K)	448	247

III. TEMPERATURE DEPENDENCE OF THE DEVONSHIRE COEFFICIENTS OF FERROELECTRICS*

by

Y.H. Tsuo

and

M.I. Bell

Physics Department

Yeshiva University

New York, New York

* Research supported by the Defense Advanced Research Projects Agency

ABSTRACT

The dielectric constants of the paraelectric phases of barium titanate and triglycine sulfate are measured as functions of temperature and applied electric field, and the results used to determine the temperature dependence of the coefficients appearing in the Devonshire expansion of the free energy. Each of the coefficients measured is found to have a linear temperature dependence, a result which is in qualitative agreement with a recently proposed generalized molecular field theory of ferroelectricity. Certain anomalies appear in the data for TGS, however, and these will require further study.

I. INTRODUCTION

According to Devonshire's thermodynamic theory of ferroelectricity[1], if a ferroelectric crystal has a center of inversion above the Curie temperature, then its free energy function G, at zero stress, can be expanded in terms of P^2. Assuming that in the ferroelectric phase the spontaneous polarization lies along the z-direction, and that electric fields are applied only along this direction so that $P=P_z$, $P_x=P_y=0$, we get

$$G=\tfrac{1}{2}AP^2 + \tfrac{1}{2}BP^4 + \frac{1}{6}CP^6 + \ldots\ldots \qquad (1)$$

where the coefficients A,B,C,....are functions of the temperature. The applied electric field is given by

$$E= \frac{\partial G}{\partial P} = AP + BP^3 + CP^5 + \ldots\ldots \qquad (2)$$

and the dielectric stiffness (reciprocal susceptibility) is

$$\chi^{-1} = \frac{\partial^2 G}{\partial P^2} = A + 3BP^2 + 5CP^4 + \ldots. \qquad (3)$$

In order to account for the Curie-Weiss law behavior of the dielectric constant, A is taken to be a linear function of temperature $A=A_o(T-T_o)$. All the higher-order Devonshire coefficients are assumed to be temperature-independent in most discussions of the thermodynamic theory.

In 1955, Drougard et al[2] studied the polarization dependence of χ^{-1} in the paraelectric phase of $BaTiO_3$ and found that B is a linear function of temperature $B=B_o(T-T_1)$. More recently, Bell and Raccah[3,4]

proposed a generalized molecular field theory of ferroelectricity (GMFT) which predicts that all the Devonshire coefficients should be linear functions of temperature. Consequently the present study was undertaken to investigate experimentally the temperature dependence of the Devonshire coefficients. We performed our experiments on barium titanate ($BaTiO_3$) and triglycine sulfate (TGS), since the phase transition is generally believed to be first order in the former and second order in the latter.

II. EXPERIMENTAL

To determine the temperature and field dependence of the dielectric stiffness above the Curie point, we use an arrangement similar to the one used by Drougard and Young[5], as shown in Fig. 1. It is basically a capacitance measurement with measuring capacitance much larger than the sample capacitance. The crystal under study is subject at the same time to a slowly varying DC biasing field and to an audio-frequency (8kHz) sine wave of constant low amplitude (about 1/300 of the coercive field).

The samples were single-crystal plates with thickness between 100 and 250 μm and area between 0.1 and 0.3 cm^2. Both surfaces perpendicular to the polar axis were completely covered with evaporated metal electrodes to avoid clamping[2]. Inside the oven, the samples were placed in a closed copper cylinder filled with helium and freely suspended by their silver lead wires. The temperature of the oven was controlled by a Leeds & Northrup Electromax III controller which provides temperature stabilization to within 0.01 ^{o}C for a period of 20 minutes or more.

In the paraelectric phase, the polarization of the sample is induced

by the biasing field applied to the electrodes. At each temperature chosen, the X-Y recorder plots the curve of χ^{-1} as a function of E^2. From Eqs. (2) and (3) we get an expression for χ^{-1} as a function of E^2,

$$\chi^{-1} = A + 3B(E/A)^2 + (-6B^2/A + 5C)\ (E/A)^4 + (21\frac{B^3}{A^2} - 26\ \frac{BC}{A} + 7D)\ (\frac{E}{A})^6 \quad (4)$$

By least-squares fitting we can determine the coefficients A,B and C. It must be remembered, however, that the susceptibility given by Eqs. (3) and (4) is the isothermal one, while the measurement conditions are adiabatic. It is easily shown[2,6] that the adiabatic and isothermal susceptibilities, χ_S and χ_T, respectively, are related by

$$\chi_S^{-1} = \chi_T^{-1} + (T/\rho\ C_p)\ (\partial E/\partial T)_P^2\ , \quad (5)$$

where ρ is the density and C_p is the specific heat at constant pressure. With the help of Eq. (2), we find

$$\chi_S^{-1} = A + 3(B + TA'^2/3\rho\ C_p)P^2 + 5(C + 2TA'B'/5\rho\ C_p)P^4 + \ldots, \quad (6)$$

where a prime is used to denote differentiation with respect to temperature. The usual assumption, that only A depends on temperature, then leads, by comparison with Eq. (3), to a correction for B,

$$\Delta B = TA_o^2/3\rho\ C_p, \quad (7)$$

and no corrections for the higher-order coefficients. The findings of Ref. 2 and the predictions of Ref. 3 would lead to corrections in the higher-order coefficients as well, e.g.

$$\Delta C = 2TA_o B_o / 5\rho\, C_p, \tag{8}$$

and so forth. It will be shown below that the corrections for C (and presumably the higher-order coefficients also) are negligible in the materials studied here.

III. RESULTS

A. Barium Titanate

Equation (4) shows that only near the Curie-Weiss temperature T_o, where the coefficient A approaches zero, can we expect to see large effects due to the nonlinear terms. In $BaTiO_3$ a first-order transition occurs at a temperature significantly above T_o, and the measured χ^{-1} is always a linear function of E^2, as shown in Fig. 2. The coefficient A has the expected linear behavior (see Fig. 3) with the values of A_o and T_o listed in Table I. As indicated in the table, our A_o agrees well with the results of others, but T_o is 10-15°C lower than generally reported[6]. Using published values of ρ and C_p in Eq. (7), we find that the adiabatic correction is approximately $\Delta B = 1.8 \times 10^{-14}$ cgs throughout the temperature range studied. Applying this correction we obtain for B the results shown in Fig. 4. The linear behavior predicted by the GMFT[3] and reported by Drougard et al[2] is evident, and least-squares fitting gives B_o and T_1 as listed in Table I. The values obtained by Drougard et al[2] are given for comparison.

B. Triglycine Sulfate

Since the phase transition in TGS is second order, measurements can be made in the paraelectric phase quite close to T_o. As a result, significant nonlinearities can be seen when χ^{-1} is plotted as a function of E^2, and this is shown in Fig. 5. For temperatures more than 2 K above T_o the relationship is essentially linear, but closer to T_o substantial contributions from terms of order E^4 and E^6 are required to fit the experimental data. (The solid curves in Fig. 5 represent least-squares fits to the measured values indicated by crosses.) The fitting gives A immediately, and the temperature dependence of this coefficient is shown in Fig. 6. The linear behavior required by the Curie-Weiss law is found, and the values of A_o and T_o, listed in Table II, are in good agreement with the results of others[7,8]. Again making use of published results for the density and specific heat,[6] we find that the adiabatic corrections for B are approximately 10% and those for C are negligible. After making the necessary corrections we obtain the results for these coefficients shown in Figs. 7 and 8. In each case the temperature dependence is linear, as predicted by the GMFT, to within the accuracy of the experiment. Least-squares fits to the forms $B = B_o(T - T_1)$ and $C = C_o(T - T_2)$ are shown in Figs. 7 and 8 and the fitting parameters listed in Table II which also gives for comparison the values of B and C obtained by Triebwasser.[8]

IV. DISCUSSION

The support given the GMFT by the results of the previous section is substantial but not complete. In the base of $BaTiO_3$, our findings differ quantitatively (but not qualitatively) from those of previous studies[2] and yield somewhat less plausible values of the parameters appearing in the GMFT.

A central assumption of the GMFT [3,4] is the replacement of the Lorentz local field $E_\ell = E + \lambda P$ by a nonlinear local field correction $E_\ell = E + \lambda_o P + \lambda_1 P^3 + \ldots$, where the local field coefficients are given by $\lambda_o = A_o T_o$, $\lambda_1 = B_o T_1$, and so forth. Our experimental results and those of Drougard et al [2] yield similar values of λ_o and λ_1, which are listed in Table III. It is worth noting that these products of experimentally measured quantities differ less between the two sets of data than do the measured quantities themselves. In addition, the values of λ_o calculated from experimental data [9] for $KNbO_3$ and $PbTiO_3$ differ by less than 25% from that of $BaTiO_3$ despite differences of as much as a factor of two in T_o and A_o. Both these results suggest that the local field corrections are in fact characteristic of the perovskite structure.

The GMFT also relates the coefficients A_o and B_o to the maximum (saturation) polarization,

$$N\mu = (3A_o/5B_o)^{\frac{1}{2}} \tag{9}$$

and the density of independent dipoles,

$$N = A_o^2/5kB_o, \tag{10}$$

where k is Boltzmann's constant. Table III lists the values of these two quantities as calculated from our experimental results and those of Drougard et al [2]. (We give N in the form of the ratio N_o/N, where

N_o is the number of unit cells per unit volume, since this is the number of unit cells required to form one of the elementary dipoles assumed by the GMFT.) The two calculated values of $N\mu$ are similar, but somewhat smaller than the 26 $\mu C/cm^2$ obtained experimentally [2]. Our data yield a significantly larger value of N_o/N than that of Drougard et al,[2] and both values are larger than the estimate $10 < N_o/N < 25$ obtained by Lambert and Comès from measurements of the diffuse scattering of x-rays.[10] Estimates based on the observed entropy change at the transition indicate, however, that the dipole length is highly variable from sample to sample and may be as great as 60 unit cells.[10] Hence, the values reported in Table III, while large, are by no means unreasonable.

In the case of TGS, we find that each of the coefficients measured has a linear temperature dependence (within experimental accuracy) throughout the temperature range investigated. Unfortunately, however, a careful examination of Eq. (4) and our experimental data shows that, due to the accidental near cancellation of several terms in the calculation, the accuracy with which the coefficients C and D can be determined from the coefficients of E^4 and E^6 is quite poor. The values obtained for D are of virtually no significance and will not be considered here. The results for C could be in error by as much as a factor of two. Further doubt is cast on the values obtained for C by the fact that using the coefficients in Table II one calculates a spontaneous polarization which has nearly saturated at room temperature, reaching a value only about one third that observed experimentally. This is due to the large and rapidly increasing value of C implied by

the linear fit shown in Fig. 8. This difficulty would disappear, however, if C were only weakly temperature dependent. Using a constant value of $C = 1.9 \times 10^{-17}$ cgs we obtain excellent agreement between the calculated spontaneous polarization and that measured by Choe et al [11], as shown in Fig. 9. This value for C, although larger than those reported by Triebwasser [8] (see Table II) and Gonzalo [7], is close to that found by Zerem and Halperin [12] (1.4×10^{-17} cgs) when they include the contribution of the coefficient D in calculating the spontaneous polarization. This value is also consistent with the GMFT, as will be shown below, and is well within the range of our experimental results.

Our experimental results for A_o and B_o in TGS, when substituted in Eqs. (9) and (10), yield strong support for the GMFT. The calculated saturation polarization is $N\mu = 4.4\ \mu C/cm^2$, in excellent agreement with the measured low-temperature value [13] of $4.3\ \mu C/cm^2$. The elementary dipole is found to have length $N_o/N = 1.1$ unit cells, in full accord with the conventional view of TGS as an order-disorder ferroelectric.

The negative value found for C_o (Table II) is inconsistent with the GMFT, however. The theory predicts

$$C_o = 99\ A_o/175\ (N\mu)^4, \qquad (11)$$

which is necessarily positive. Fortunately, the value required above to obtain good agreement with the observed spontaneous polarization ($C = 1.9 \times 10^{-17}$ cgs, independent of temperature) is con-

sistent with both Eq. (11) and the predicted temperature dependence,

$$C = C_o(T - T_2). \tag{12}$$

If the value quoted for C is assumed correct at $T = T_o$, then Eqs. (11) and (12) can be solved for T_2, yielding $T_2 = 46$ K. The small value of T_2, when used in Eq. (12), guarantees that C is weakly temperature dependent, varying by only 10% over the temperature range in which the spontaneous polarization was fitted (Fig. 9).

While it is clearly necessary to develop more accurate methods of determining the high-order Devonshire coefficients in order to test the temperature dependence predicted by the GMFT, all of our results are consistent with that theory, and the most reliable of them provide strong new evidence for its validity.

REFEKENCES

1. A.F. Devonshire, Advan. Phy. 3, 85 (1954).
2. M.E. Drougard, R. Landauer, and D.R. Young, Phys. Rev. 98, 1010 (1955); See also, M.E. Drougard and E.J. Huibregtse, IBM J. Res. and Devel. 1, 318 (1957).
3. M.I. Bell and P.M. Raccah, Technical Report ECOM-74-0407-1, Yeshiva University (1975).
4. M.I. Bell and P.M. Raccah, Bull. Am. Phys. Soc. 20, 349 (1975).
5. M.E. Drougard and D.R. Young, Phys. Rev. 94, 1561 (1954).
6. E. Fatuzzo and W.J. Merz, Ferroelectricity (J. Willey and Sons, New York, 1967).
7. J.A. Gonzalo, Phys. Rev. 144, 662 (1966).
8. S. Triebwasser, IBM J. Res. Develop. 2, 212 (1958).
9. S. Triebwasser, Phys. Rev. 101, 993 (1956); J.P. Remeika and A.M. Glass, Mat. Res. Bull. 5, 37 (1970).
10. M. Lambert and R. Comes, Solid St. Comm. 7, 305 (1969).
11. H.M. Choe, J.H. Judy, and A. Van der Ziel, Ferroelectrics 15, 181 (1977).
12. J.Z. Zerem and A. Halperin, Ferroelectrics 7, 205 (1974).
13. A.G. Chynoweth, Phys. Rev. 117, 1235 (1960).

Table I. Devonshire coefficients of $BaTiO_3$ found in the present study and those reported by Drougard et al (Ref. 2).

	Present work	Reference 2
$A(10^{-5}$ cgs)	7.3 (T - 369.4K)	7.6 (T - 378K)
$B(10^{-14}$ cgs)	2.3 (T - 406K)	1.8 (T - 448K)

Table II. Devonshire coefficients of TGS found in the present study and those reported by Triebwasser (Ref. 8).

	Present work	Reference 8
$A(10^{-3}$ cgs)	3.57 (T - 321.8 K)	3.92 (T - 323K)
$B(10^{-10}$ cgs)	12.5 (T - 277 K)	8.0
$C(10^{-17}$ cgs)	-8 (T - 324 K)	0.5

Table III. Parameters of the generalized molecular field theory for $BaTiO_3$ (see text) as calculated from the results of the present work and those of Drougard et al (Ref. 2).

Parameter	Present work	Reference 2
$\lambda_o (10^{-2})$	2.7	2.9
$\lambda_1 (10^{-12})$	9.3	8.1
$N\mu (\mu C/cm^2)$	14	17
N_o/N	50	33

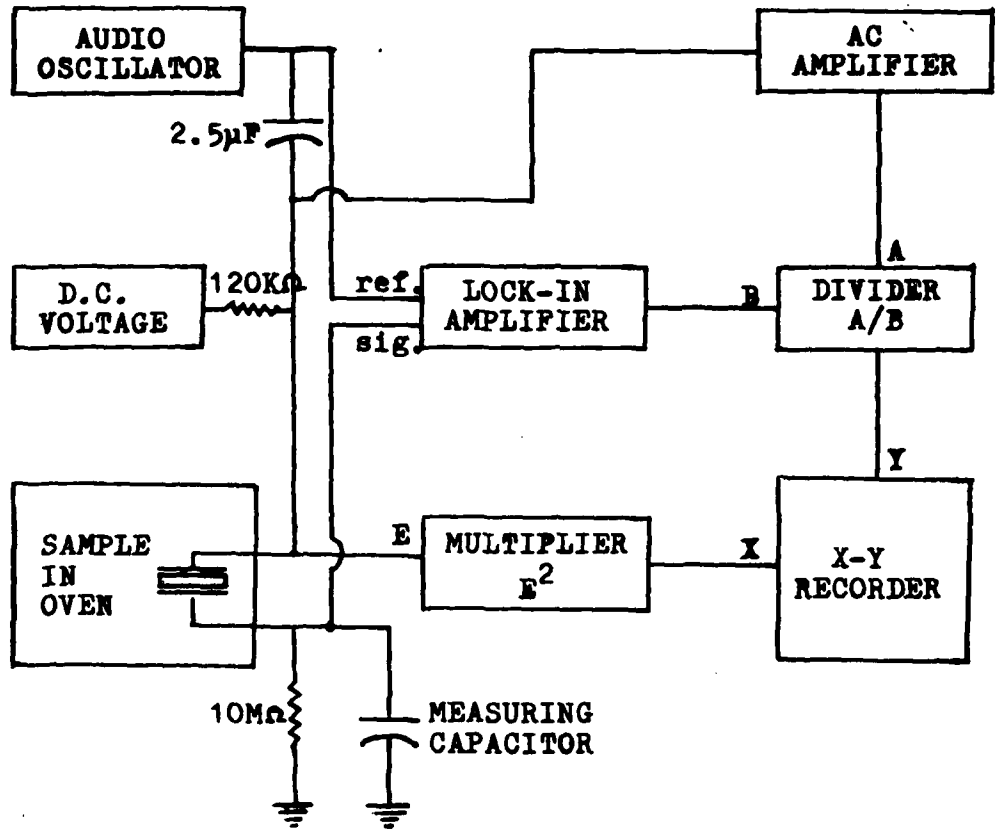

Fig. 1. Apparatus for recording the dielectric stiffness as a function of the temperature and the square of the applied electric field.

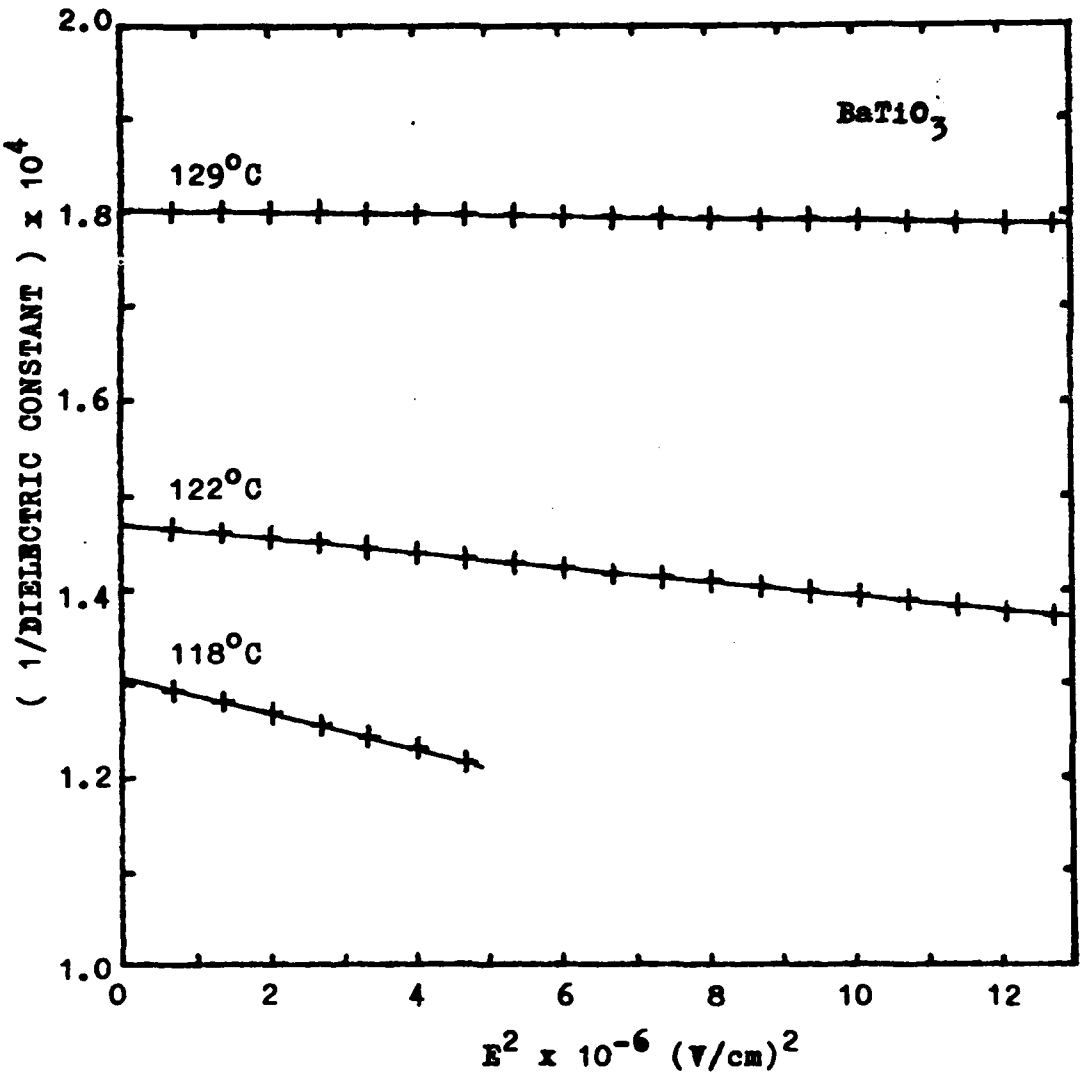

Fig. 2. The dielectric stiffness χ^{-1} of $BaTiO_3$ as a function of the square of the applied electric field for several temperatures above the ferroelectric-paraelectric transition.

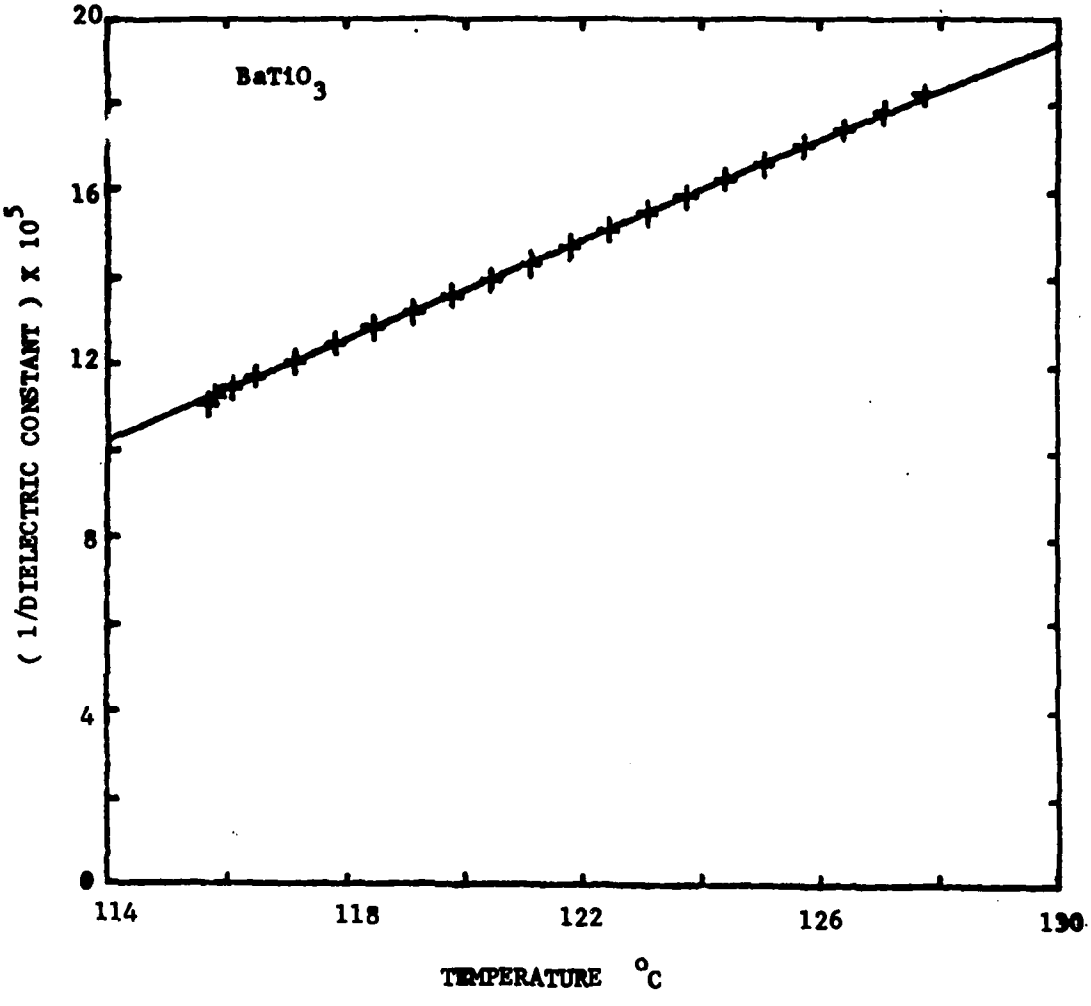

Fig. 3. The first Devonshire coefficient A as a function of temperature in $BaTiO_3$.

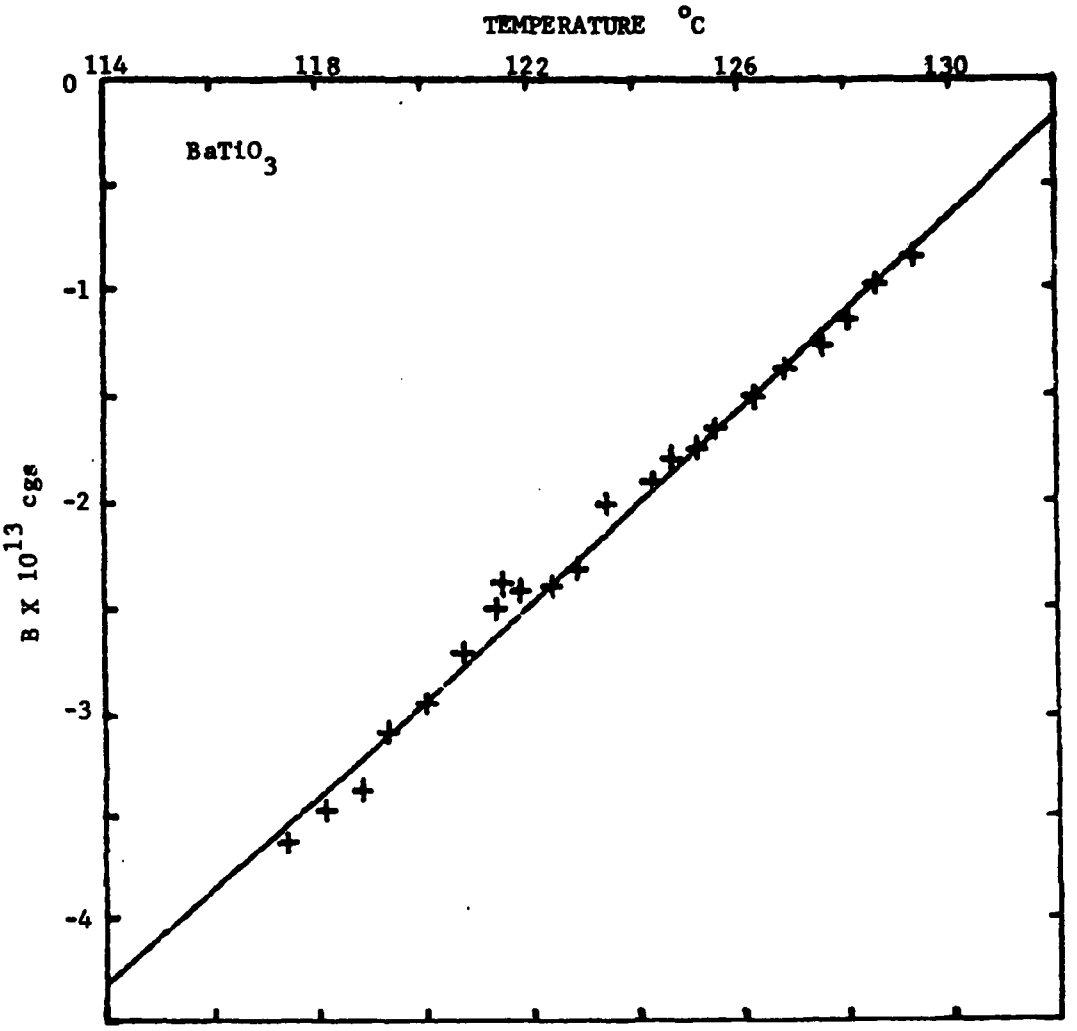

Fig. 4. The second Devonshire coefficient B as a function of temperature in $BaTiO_3$.

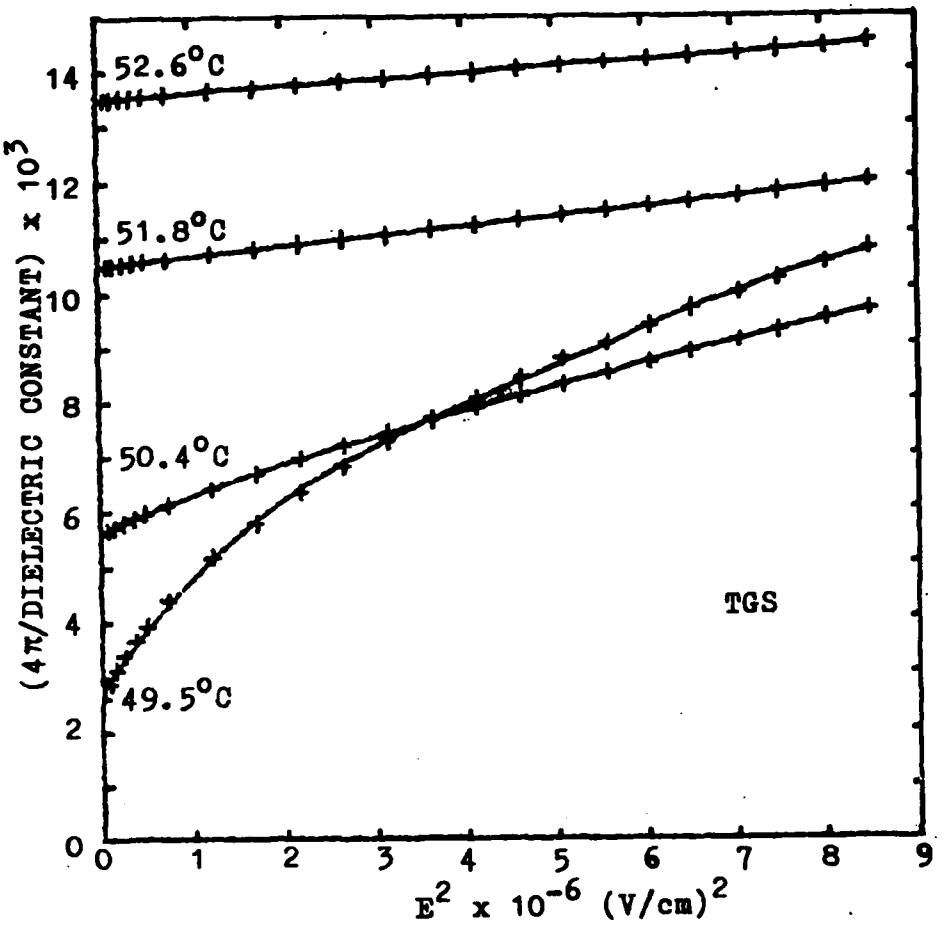

Fig. 5. The dielectric stiffness χ^{-1} of TGS as a function of the square of the applied electric field for several temperatures above the ferroelectric-paraelectric transition.

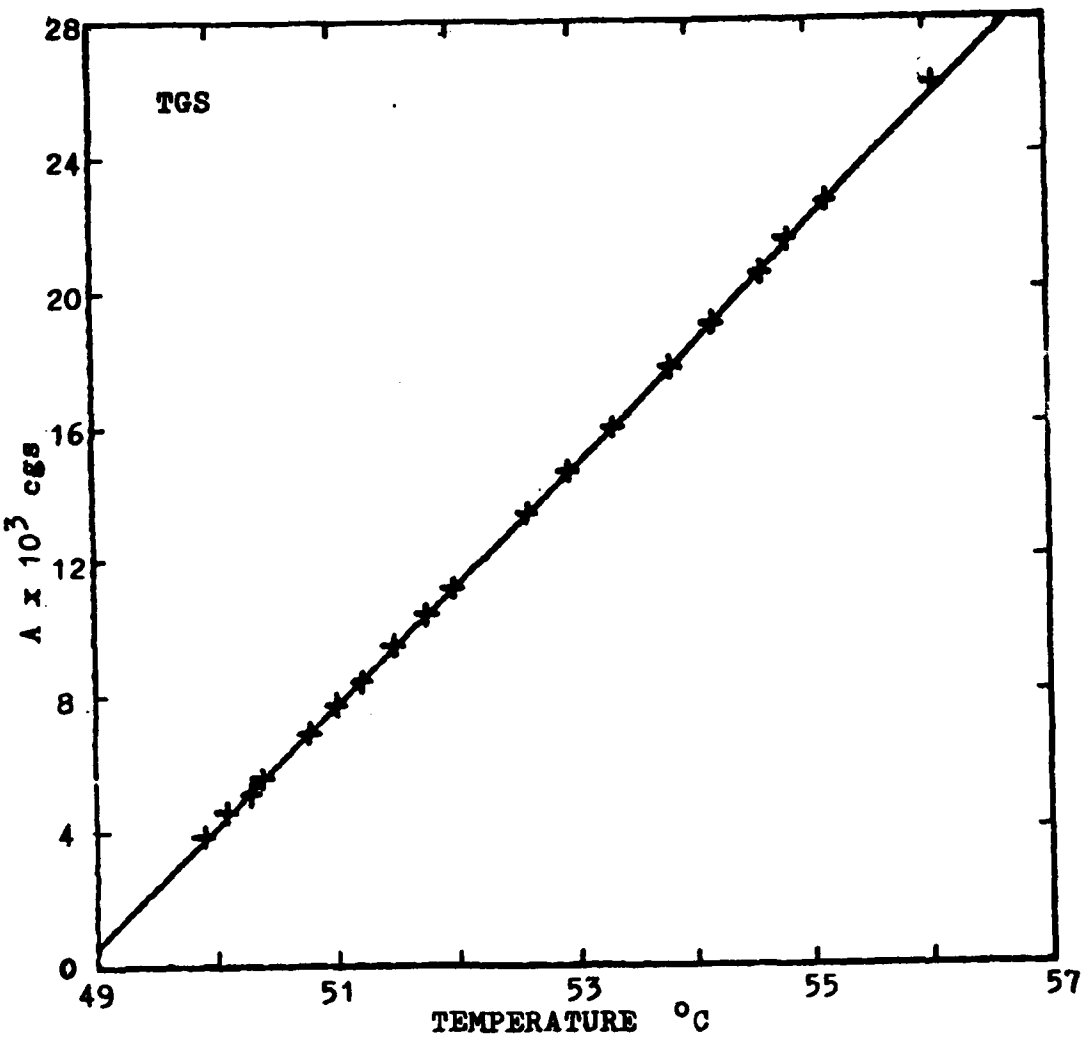

Fig. 6. The first Devonshire coefficient A as a function of temperature in TGS.

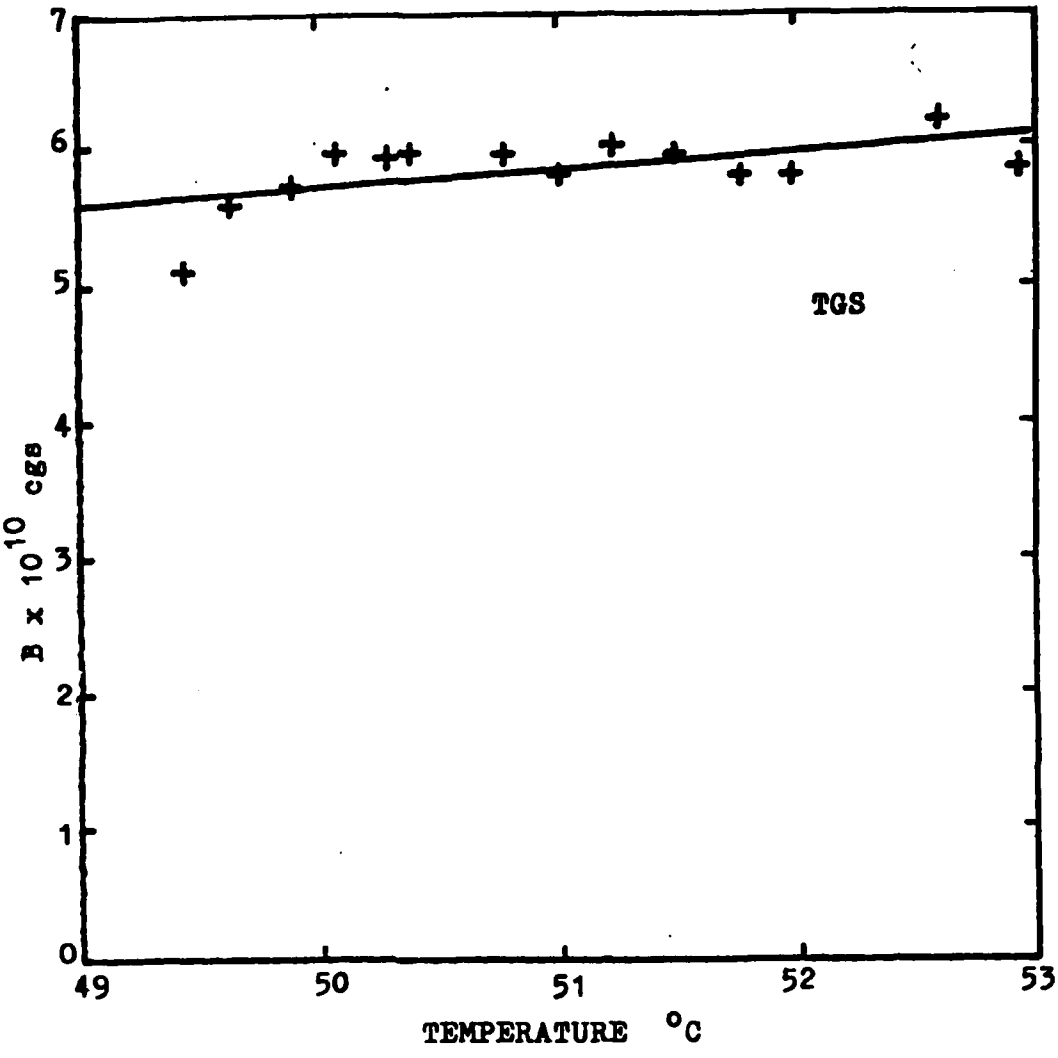

Fig. 7. The second Devonshire coefficient B as a function of temperature in TGS.

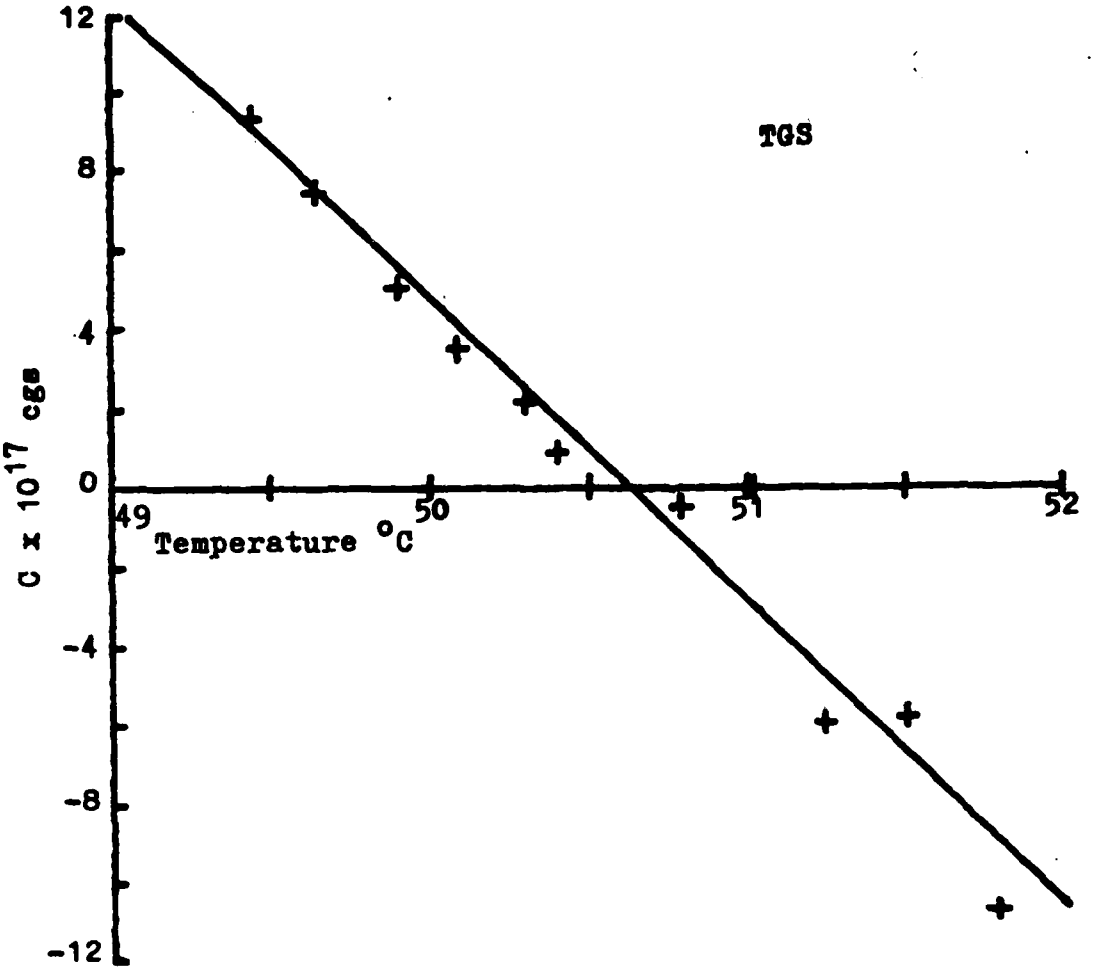

Fig. 8. The third Devonshire coefficient C as a function of temperature in TGS.

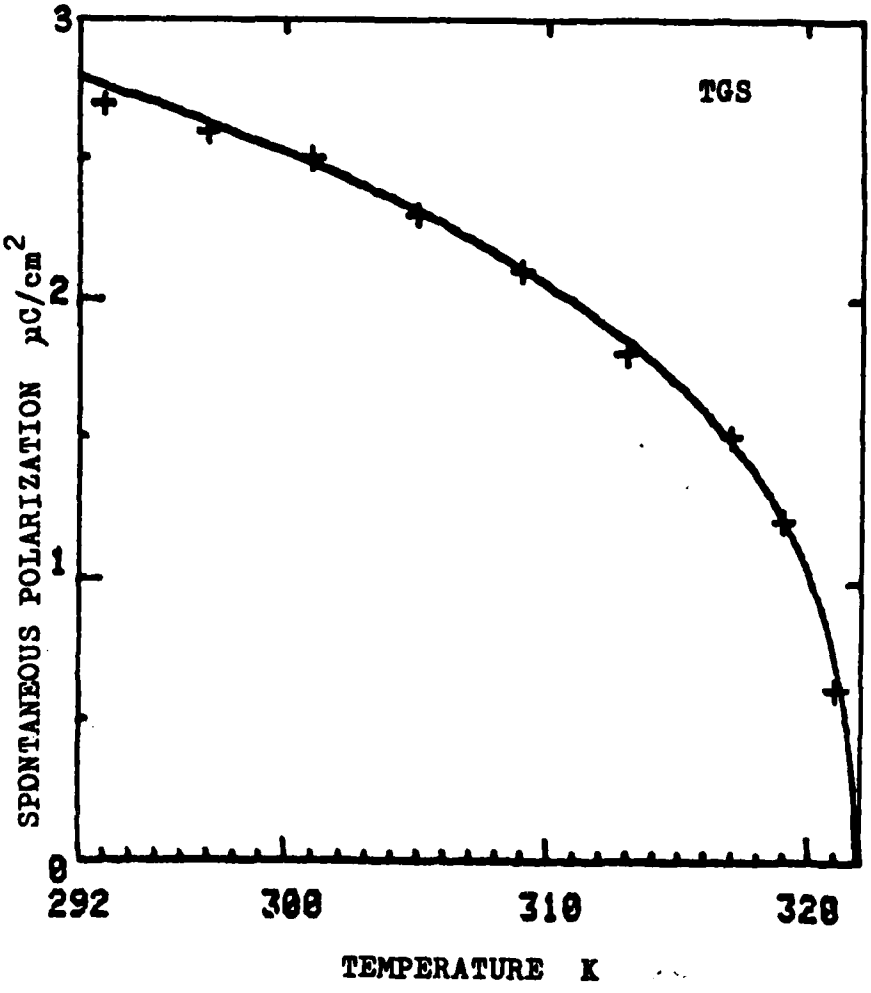

Fig. 9. Measured spontaneous polarization of TGS (crosses, Ref. 11) compared with values calculated using A and B from Table II and $C = 1.9 \times 10^{-17}$ cgs (solid curve).

IV. PERFORMANCE OF IMPROPER FERROELECTRICS IN PYROELECTRIC VIDICON APPLICATIONS*

by

M.I. Bell

Physics Department
Yeshiva University
New York, New York

* Research supported by the Defense Advanced Research Projects Agency

I. INTRODUCTION

It is the purpose of this note to review the known limitations on the performance of ferroelectric materials as pyroelectric vidicon targets and to demonstrate, both theoretically and experimentally, that a relatively new class of materials, the improper ferroelectrics, can avoid these limitations and may eventually yield better performance than the materials now in use. We first introduce the material figure of merit, which is proportional to the signal-to-noise ratio obtainable from a given material when used as a vidicon target. We then extend previous results[1] to show that the estimated upper limit for the figure of merit originally obtained on the basis of a particular model for ferroelectric phase transitions is in fact a property of a large class of generalized molecular field models. When the temperature dependence of the figure of merit is examined, using both the generalized molecular field theory[2] (GMFT) and the Devonshire formalism[3], we find that when either of these theories applies the performance of a vidicon target can be expected to deteriorate as its Curie temperature is approached, despite a large increase in its pyroelectric coefficient. Finally, we take note of a class of materials, the improper ferroelectrics, to which these considerations do not apply and for which a radically different temperature dependence of the figure of merit is predicted. Preliminary experimental results[4] confirm this theoretically predicted behavior and indicate that a well-known improper ferroelectric (terbium molybdate) has a figure of merit near its transition temperature which would make it competitive with the best of the materials now in use as vidicon targets.

II. FIGURE OF MERIT

It is well known[5] that the signal-to-noise ratio of a pyroelectric vidicon depends on the properties of the target material through the ratio

$$M = p/\epsilon c \tag{1}$$

where p is the pyroelectric coefficient, ϵ is the dielectric constant, and c is the volume specific heat. In the following treatment of the figure of merit M, we will not consider the specific heat in any detail, since its variations, both with temperature and from one material to another, are small compared to those exhibited by the pyroelectric coefficient and dielectric constant. It is also convenient to replace the dielectric constant by the susceptibility $\chi = \epsilon - 1$, an approximation which is quite reasonable in view of the large values of ϵ typical of ferroelectrics. Using these approximations, we are able to investigate the behavior of the figure of merit M by studying the ratio

$$m = p/\chi, \tag{2}$$

which, as we have noted previously[6], is quite easily calculated from most models for ferroelectric phase transitions.

III. LOCAL FIELD MODELS

We have reported elsewhere[1] that the existence of a ferroelectric crystal with a value of M significantly greater than 3.1×10^4 cm^2/C is most improbable. (The largest value reported to date[5] is that of

triglycine fluoberyllate, 9.5×10^3 cm^2/C.) This estimated upper limit is based on consideration of a local (or molecular) field model which has been described in detail in previous reports.[2,6,7] We can now show that a large class of local field models, which includes the model used in our earlier work, yields an expression for the figure of merit identical to that obtained in the special case studied previously. This result strengthens our belief that proper ferroelectrics to which such models apply offer little hope for improved pyroelectric vidicon targets.

In a local field model of a ferroelectric phase transition we represent the crystal by an ensemble of N electric dipoles per unit volume, where each dipole has a moment μ, and the dipoles interact via a local field

$$E_\ell = E + \lambda(P), \tag{3}$$

where E is the macroscopic (applied) field, and the local field correction $\lambda(P)$ is an arbitrary function of the polarization P. In order to apply the techniques of statistical mechanics to such a system, it is necessary to specify which relative orientations of the local field and dipole moment are permitted. One then obtains a relation of the form

$$P = N\mu\, f(x), \tag{4}$$

where $x = \mu E_i/kT$, and the form of $f(x)$ is determined by the allowed orientations of the dipole in the local field. Thus, a particular local field model is obtained by specifying the polarization dependence of the local field, i.e. $\lambda(P)$, and the permitted dipole orientations, i.e. $f(x)$. Our previous work[2,6,7] has dealt with local fields which have the form of a power series $\lambda(P) = \lambda_o P + \lambda_1 P^3 + \lambda_2 P^5 + \ldots$ or the closely related Padé approximant $\lambda(P) = \lambda_o P/[1-(\lambda_1/\lambda_o)P^2]$, and with classical ("infinite spin") systems in which the dipoles can have any orientation relative to the local field, so that $f(x)$ is the Langevin function $\coth x - 1/x$.

For an arbitrary local field model, we can investigate the ratio $m = p/\chi$ by using the relation

$$m = (\partial E/\partial T)_P, \tag{5}$$

which follows from elementary thermodynamics.[6] (Note, however, that the susceptibility χ in Eq. (5) is the isothermal one and that adiabatic corrections may then be needed to predict the performance of an actual vidicon target.[1]) Assuming that the local field correction $\lambda(P)$ has no explicit temperature dependence, Eqs. (3)-(5) yield

$$m = kx/\mu. \tag{6}$$

Equation (6) is the relation which was obtained previously for the GMFT and which led to the estimated upper limit for M cited above. We now see that this result is more general than originally supposed and applies to all local field models.

IV. TEMPERATURE DEPENDENCE OF THE FIGURE OF MERIT

The general result (5) can also be used to study the temperature dependence of the figure of merit. If we wish to use a local field model, then Eq. (6) applies as well. In each of the local field models studied to date,[2,6,7] we have found that $x = f^{-1}(P/N\mu)$ is a monotonically increasing function of P, which vanishes at $P = 0$. (We expect that x will have these properties in all physically reasonable local field models, and work is under way to explore these and other general characteristics of local field models.) Thus, in every local field model studied so far the figure of merit (or more precisely, the ratio m) is found to decrease as the Curie temperature is approached and the spontaneous polarization decreases.

A similar result is obtained from Devonshire's phenomenological theory of ferroelectricity.[3] If the free energy is expanded as a power series in the polarization,

$$G = \tfrac{1}{2} AP^2 + \tfrac{1}{4} BP^4 + \frac{1}{6} CP^6 + \ldots, \tag{7}$$

then the electric field, $E = (\partial G/\partial P)_T$, is

$$E = AP + BP^3 + CP^5 + \ldots, \tag{8}$$

and Eq. (5) yields

$$m = A'P + B'P^3 + C'P^5 + \ldots, \tag{9}$$

where a prime indicates differentiation with respect to temperature. It is usual, in applying the Devonshire formalism, to assume that A has the form $A_o(T-T_o)$ and that the other coefficients are temperature independent. This leads to the simple relation

$$m = A_o P. \tag{10}$$

(The corresponding result for zero applied field, $m = A_o P_s$, where P_s is the spontaneous polarization, has been obtained elsewhere[8] under more restrictive assumptions.) While Eq. (10) clearly predicts a monotonic decrease in m at zero field as the Curie temperature is approached, the question of the temperature dependence of the higher-order Devonshire coefficients is by no means resolved.[9] The available experimental evidence indicates that these coefficients are in fact temperature dependent, but that the observed dependences are at least consistent with the prediction of the GMFT that all the coefficients A', B', C',... are positive, so that Eq. (9) also leads to a monotonically decreasing m.

Finally, a direct measurement[4] of the temperature dependence of the figure of merit M in triglycine sulfate (TGS) lends strong support to our theoretical expectations. Using dynamic response measurements of the type originated by Chynoweth[10] and further developed by Simhony and Shaulov,[11] one can obtain a pyroelectric signal (voltage) which is directly proportional to M. This technique, which will be described in detail elsewhere, eliminates the need to calculate products or ratios of independent measurements, a process

which can lead to serious errors, especially in temperature ranges where the properties involved are strongly temperature dependent. The result for TGS is given in Fig. 1 and clearly shows the expected behavior. The small rise in M just above room temperature results from a reduction in the pyroelectric voltage at lower temperatures due to loading by the input capacitance of the measuring amplifier and is completely eliminated when one corrects the data for this effect. Since the coefficients B', C',... in Eq. (9) are not known, measurements of this type can yield valuable information of a fundamental nature as well as predictions of vidicon target performance.

V. IMPROPER FERROELECTRICS IN VIDICON APPLICATIONS

The considerations of the previous sections indicate that among ferroelectrics to which the Devonshire or local field theories apply, one is unlikely to obtain a material with a significantly larger room temperature figure of merit than those now in use. In addition, attempts to improve performance by operating the target close to its Curie temperature, where the pyroelectric coefficient is large, must fail due to the temperature dependence of M predicted by Eqs. (6) and (9) and reflected in the data of Fig. 1. The decrease in the figure of merit as the Curie temperature is approached can be regarded as a consequence of the fact that while both the dielectric constant and pyroelectric coefficient increase dramatically near the ferroelectric-to-pyroelectric transition, a free energy of the form (7) will always require that the dielectric constant dominate the ratio. However, in recent years there has been considerable interest in an unusual class

of ferroelectrics which cannot be described by the free energy (7) and which typically exhibit only a small increase in dielectric constant near the phase transition. These improper or extrinsic ferroelectrics have been the object of much theoretical and experimental investigation,[12] and it has been suggested [13] that, without a large increase in dielectric constant to compete with the increase in pyroelectric coefficient, these materials might exhibit substantial increases in figure of merit as the transition temperature is approached. In the following, we will demonstrate both theoretically and experimentally, that this suggestion is correct and could lead to major improvements in pyroelectric vidicon performance.

From a theoretical point of view, the distinguishing feature of an improper ferroelectric is that the order parameter which describes the spontaneous symmetry change at the paraelectric-ferroelectric phase transition [14] is neither the spontaneous polarization nor any other quantity having the same transformation properties.[12] Instead, a polarization appears at the transition temperature as a result of coupling between the order parameter (or soft mode) and the polarization (or polar optical mode). This coupling can be described in macroscopic terms by using a free energy which has been expanded as a power series in both the order parameter η and the polarization P and which contains coupling terms proportional to products of η and P. The simplest such free energy has been treated by Dvorak [15] and has the form (at zero stress)

$$G = \tfrac{1}{2} A(T-T_o)\ \eta^2 + \tfrac{1}{4} b\eta^4 + \frac{1}{6} c\ \eta^6 + \ldots$$

$$+ \tfrac{1}{2} \chi_o^{-1}\ P^2 + f\eta^n P. \qquad (11)$$

The electric field $E = (\partial G/\partial P)_T$ is given by

$$E = \chi_o^{-1}\ P + f\eta^n, \qquad (12)$$

and applying Eq. (5) yields

$$m = nf\eta^{n-1}(\partial\eta/\partial T)_P. \qquad (13)$$

The derivative in Eq. (13) can be evaluated by noting [15] that the spontaneous value of the order parameter η_s is given by $(\partial G/\partial\eta)_T = 0$ or

$$a(T-T_o) + b\eta_s^2 + c\eta_s^2 + nf\eta_s^{n-2}\ P = 0. \qquad (14)$$

If we differentiate Eq. (14) with respect to T and substitute in (13), assuming E = 0, we obtain

$$m = -naf\eta_s^{n-2}/[2(b+4c\eta_s^2) - n(n-2)\ f^2\chi_o\eta_s^{2(n-2)}]. \qquad (15)$$

Although the temperature dependence of (15) is not obvious, a particularly simple case is provided by the rare-earth molybdates of the form $R_2(M_oO_4)_3$, where R = Gd, Tb, Sm, etc. In this case

the appropriate free energy is obtained [15] for n = 2, and Eq. (15) becomes

$$m = - af/(b+2c\ \eta_s^2). \tag{16}$$

It is readily shown [15] that the stability of the ferroelectric phase requires both c and $b + 2c\ \eta_s^2$ to be positive. Hence, m has a maximum at the minimum of η_s, and this presumably occurs at the Curie temperature.

Thus, in sharp contrast to the case of proper ferroelectrics, we expect the figure of merit of a rare-earth molybdate to increase as the transition temperature is approached. Figure 2 shows M as measured [4] in terbium molybdate (TMO) by the dynamic response technique. A detailed discussion of the results for TMO and several other molybdates will be given elsewhere. In the present context it is sufficient to note that the figure of merit of TMO rises from a room-temperature value of about 350 cm^2/C to a peak at the Curie temperature greater than 6000 cm^2/C. This dramatic increase gives it a figure of merit greater (in a limited temperature range) than that of TGS and approaching that of the best available material, triglycine fluoberyllate. The rare-earth molybdates were chosen for this preliminary work because they are readily available and widely studied. No attempt was made to select or modify the material to achieve a large figure of merit. For this reason we believe that the potential of improper ferroelectrics for improved pyroelectric vidicon target materials is largely untapped and that

further investigation along these lines is likely to be very rewarding.

REFERENCES

1. M.I. Bell and P.M. Raccah, IEDM Tech. Digest, 70 (1975).
2. M.I. Bell and P.M. Raccah, Bull. Am. Phys. Soc. 20, 359 (1975); see also Chapter II.
3. A.F. Devonshire, Advan. Phys. 3, 85 (1954).
4. A. Shaulov and M.I. Bell, unpublished results.
5. L.E. Garn and E.J. Sharp, IEEE Trans. Parts, Hybrids, and Packaging PHP-10, 208 (1974); B. Singer and J.J. Lalak, Final Report on Contract No. DAAK02-74-C-0054, Philips Laboratories, Briarcliff Manor, N.Y. (1975).
6. M.I. Bell and P.M. Raccah, Technical Report ECOM-74-0470-1, Yeshiva University (1975).
7. M.I. Bell and P.M. Raccah, Technical Report ECOM-74-0470-2, Yeshiva University (1975).
8. H.M. Choe, J.H. Judy, and A. van der Ziel, Ferroelectrics 15, 181 (1977).
9. See Chapter III and Appendix B.
10. A.G. Chynoweth, J. App. Phys. 27, 78 (1956).
11. H. Simhony and A. Shaulov, J. App. Phys. 42, 3741 (1971); 43, 1440 (1972).
12. See, for example, A.P. Levanyuk and D.G. Sannikov, Sov. Phys.-Usp. 17, 199 (1974).
13. L.E. Cross, private communication.
14. L. Landau, Collected Papers, ed. by D. ter Haar (Gordon and Breach, New York, 1965) p. 193.
15. V. Dvorak, Ferroelectrics 7, 1 (1974).

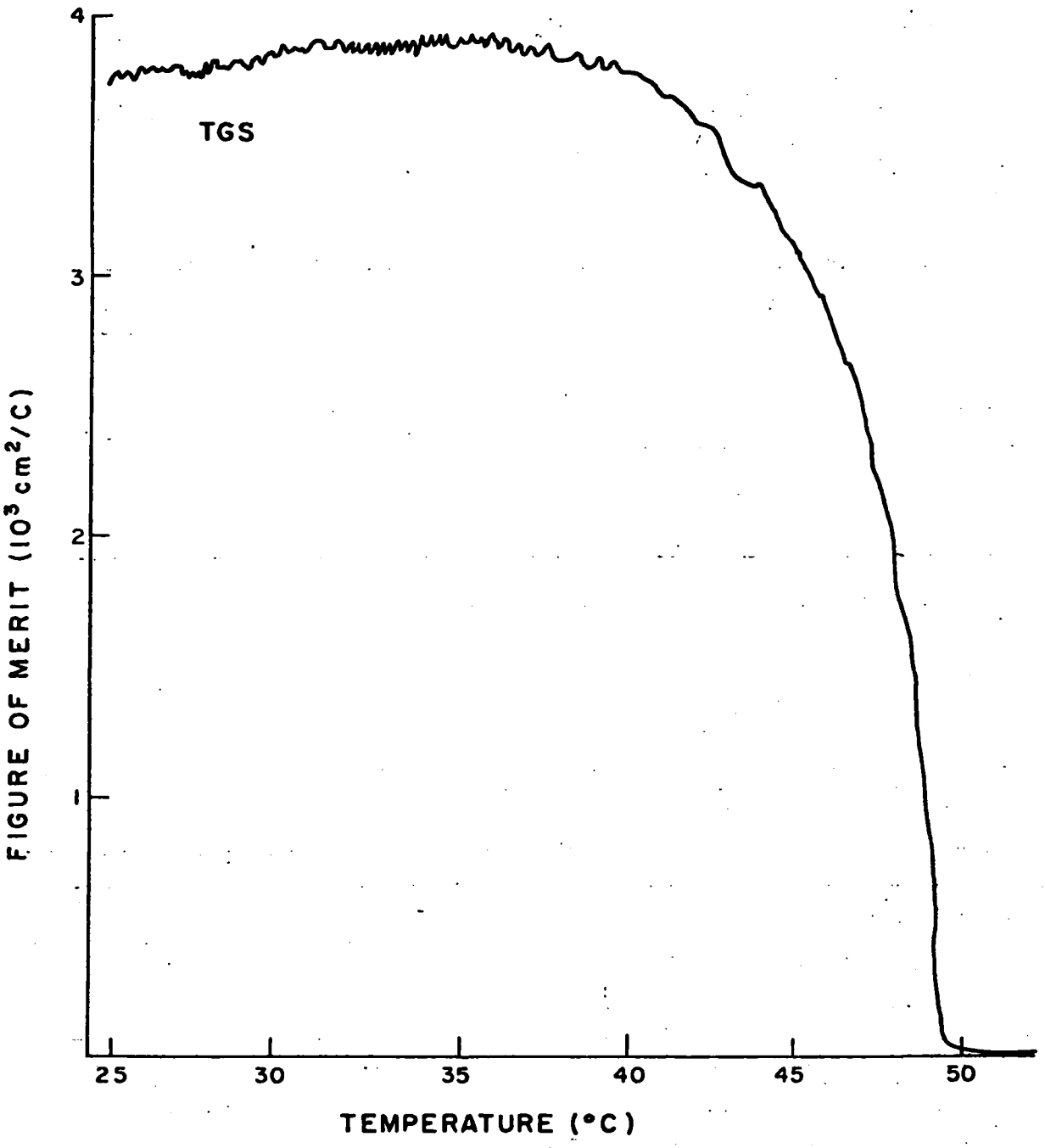

Fig. 1. Vidicon target figure of merit $p/\varepsilon\varepsilon_o c$ for triglycine sulfate.

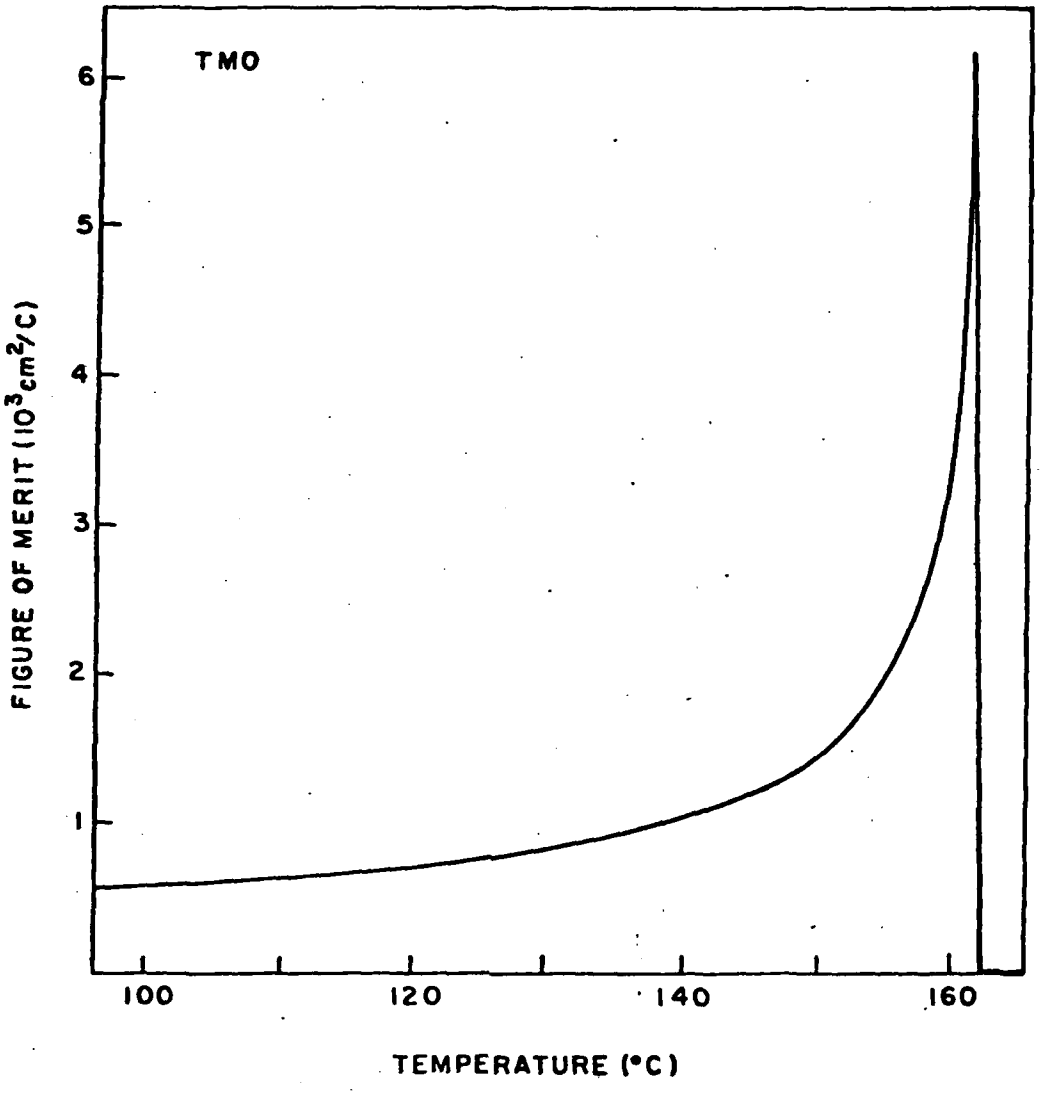

Fig. 2. Vidicon target figure of merit $p/\varepsilon\varepsilon_o c$ for terbium molybadate.

V. FERROELECTRIC MATERIALS FOR ENERGY CONVERSION*

by

Y.H. Tsuo

and

M.I. Bell

Physics Department

Yeshiva University

New York, New York

* Research supported by the Defense Advanced Research Projects Agency

ABSTRACT

A study of the published literature on ferroelectric thermal to electrical energy conversion provides the basis for classifying proposed ferroelectric converters into three types, based on their distinctly different principles of operation. These types are designated thermodielectric, pyroelectric, and pyro-ferroelectric, and a figure of merit is derived for each, permitting an assessment of the relative merit of various ferroelectric materials when used in converters of each type. Results from various theories of ferroelectricity and from the experimental literature are used to evaluate and compare these figures of merit, and an attempt is made to identify promising directions for future studies aimed at achieving efficient thermal to electrical energy conversion using ferroelectrics.

I. Introduction

The advantages of using ferroelectric materials for the conversion of heat energy directly into electrical energy are that they are radiation resistant, they can produce high voltage outputs so that there is no need for up-conversion, they can produce either AC or DC output, they have flat spectral responses, and they can have very high specific outputs (i.e. power output per unit weight). The disadvantages of ferroelectric converters are that they require a periodic heat source and the absolute conversion efficiencies are low. The ferroelectric converters considered to date can be classified into three types, thermodielectric, pyroelectric, and pyro-ferroelectric, according to their different operating principles.

II. Thermodielectric Converter

Heat conversion can be accomplished with any charged capacitor in which the permittivity of the dielectric varies with temperature. A typical circuit of a thermodielectric converter is shown in Fig. 1. The dielectric material in the parallel-plate capacitor is normally, although not necessarily, a ferroelectric material. The capacitor is initially charged by the storage battery through the charging diode. At the Curie temperature T_c the capacitance is a maximum because of the large dielectric constant ϵ_c. The charge on the capacitor is $Q = CV$, where V is the storage battery voltage. If the capacitor is cooled to T_a or heated to T_b, the dielectric constant drops to ϵ_a or ϵ_b, and the capacitance drops by a factor ϵ_a/ϵ_c or ϵ_b/ϵ_c. The excess charge which appears at the capacitor due to the drop in capacitance will be discharged through the

discharge diode and load the storage battery, thus completing a thermal to electrical energy conversion cycle.

In 1959, S.R. Hoh first established the feasibility of thermodielectric energy converters using ferroelectric materials [1-3]. In 1961, Clingman and Moore [4] calculated the theoretical conversion efficiency for polycrystalline $BaTiO_3$ and found that it is in the range of 0.5% to 1%. Childress [5] considered the sharper phase transitions of poled single crystals of $BaTiO_3$, included the field induced phase transition, and found an efficiency of 0.5%. In 1963, S.R. Hoh [6] reviewed the subject and, instead of using the parameters of $BaTiO_3$, chose a set of idealized material parameters and found an efficiency of 5.6%. Hoh also did some experimental work and tried to use thin films, but was unable to prepare suitable ferroelectric films. In 1968, L. Eyraud [7] and J. Perrigot [8] in France also studied the thermodielectric converter. Recently, in 1976, Pulvari and Garcia [9] proposed the use of a multiple-layer structure to achieve higher dielectric breakdown and possibly a higher conversion efficiency.

Analysis [4] of the efficiency of the thermodielectric converter leads to consideration of the ratio CE_b^2/c, where C is the Curie constant E_b is the dielectric strength (breakdown field), and c is the volume specific heat. The larger this figure of merit, the better a material will perform in a thermodielectric converter. Using published values for the parameters of $BaTiO_3$, one finds [4] that the figure of merit is 3.1×10^{15} $V^2 cmK^2/cal$. A realistic efficiency [3] for a $BaTiO_3$ thermodielectric converter is about 10^{-3}; a practical converter would require a material with a figure of merit at least an order of magnitude greater than that of $BaTiO_3$.

III. Pyroelectric Converter

A pyroelectric converter (Fig. 2) uses the pyroelectric effect to generate electrical power. The incoming light is chopped and the variation in sample temperature is small, with the temperature of the material remaining below the transition temperature. This technique was considered by L.J. Sivian [10] as early as 1942, and in 1974 A. van der Ziel showed [11], by using a small-signal model, that the conversion efficienty is small (0.025%) for most pyroelectric materials. From van der Ziel's derivation we see that the influence of material parameters on the conversion efficiency is proportional to p^2/ce, where p is the pyroelectric coefficient, c is the volume specific heat, and e is the dielectric constant. We shall use this quantity, p^2/ce, as the application figure of merit for pyroelectric energy conversion materials.

IV. Pyro-ferroelectric Converter

The pyro-ferroelectric converter operates with the same principle as the pyroelectric converter except that the variation in temperature is large, and the ferroelectric material is heated very close to the transition temperature T_c, but kept slightly below to avoid depoling. This achieves maximum utilization of the spontaneous polarization. Because the variation in temperature is large, the small-signal theory as was used by van der Ziel in calculating the efficienty of pyroelectric converter is not valid in this case. Gonzalo [12] analyzed the stored and the convertible energy of ferroelectrics from the point of view of their basic electrostatic, thermal and transport properties, and he concluded that ideal efficiencies of the order of 10 - 15% could be attained if proper materials are developed to be used in multistage pyro-ferroelectric converters.

According to Gonzalo, the conversion efficiency of a single stage pyro-ferroelectric converter using second (or close to second) order proper ferroelectrics, neglecting strain energy, is $\eta = 2\pi P_s^2/C\bar{c}$ (cgs units.) where C is the Curie constant, $\bar{c}$ is the average volume specific heat over ΔT, and P_s is the spontaneous polarization at the temperature $T_c - \Delta T$, with the requirement that dP_s^2/dT is constant within ΔT. Obviously, we can use the quantity $P_s^2/C\bar{c}$, which is equal to $\eta/2\pi$, as the application figure of merit for proper ferroelectrics used as pyro-ferroelectric energy conversion materials. For the material $NaNO_2$, with $\Delta T = 5$ K Gonzalo found a conversion efficiency of 0.2% and a specific output of 4.4×10^3 W/lb (if $\Delta T = 75$ K then one obtains 3% and 1.5×10^7 W/lb).

V. New Directions and Materials

The figure of merit $p^2/c\epsilon$ which determines the efficiency of a pyroelectric converter (Section III) might be expected to increase at temperatures near a ferroelectric-to-paraelectric phase transition where the pyroelectric coefficient p increases sharply. Unfortunately, in most ferroelectrics the dielectric constant ϵ also increases near the phase transition, and it can be shown [13] that in proper ferroelectrics, to which the usual Devonshire theory [14] applies, the ratio $p/(\epsilon-1)$ is proportional to the spontaneous polarization P_s and so is a decreasing function of temperature. In recent years, another class of ferroelectric phase transitions has been identified, however, in which the polarization is not the order parameter.[15] Such improper ferroelectrics generally have a dielectric constant which is weakly temperature dependent,

often exhibiting only a small discontinuity at the Curie point. As we have noted elsewhere,[16] this behavior can lead to large values of p/ϵ near the transition, and recent measurements[17] on several rare-earth molybdates have confirmed this. Typical results (for gadolinium molybdate, $Gd_2(MoO_4)_3$, a few tenths of a degree below T_c) yield $p^2/\epsilon c = 1.1 \times 10^{-17}$ C^2/J cmK, a value nearly 2.5 times greater than used by van der Ziel in his efficiency estimate.[11] Obviously, this figure of merit is still far too small to produce an efficient converter, but the rare-earth molybdates comprise only the first of many families of improper ferroelectrics whose unusual properties are still under investigation, and there is as yet no reason to believe that very much greater values of $p^2/\epsilon c$ will not be found.

A second remarkable property of certain improper ferroelectrics forms the basis of a novel energy converter which would not, in general, be feasible using proper ferroelectrics. We have recently observed[17] that despite repeated cycling through the ferroelectric-paraelectric phase transition, an essentially single-domain sample of a rare-earth molybdate will retain its original direction and magnitude of spontaneous polarization. Levanyuk and Sannikov[15] have pointed out on theoretical grounds that for an improper ferroelectric such transitions from a paraelectric to a single-domain ferroelectric state need not be as energetically unfavorable as in a proper ferroelectric. A small amount of elastic energy, perhaps due to clamping or internal strains, might be sufficient to stabilize the single-domain state. With the possibility of depoling eliminated in this way, we may consider energy conversion cycles in which the

temperature passes through the transition temperature. Only the simplest and most obvious such cycle will be considered here. Refinements are likely to lead to improved efficiency.

Let us suppose that a slab of improper ferroelectric in the form of a parallel-plate capacitor with area A and thickness d is heated through a first-order phase transition by an incident radiation flux F, and then cooled back through the transition by interrupting the flux. If this process is repeated continuously, it is readily shown [18] that when steady state conditions are achieved, the time required for a complete heating and cooling cycle is $\tau = 4d\Delta Q/F$, where ΔQ is the net heat absorbed (emitted) per unit volume during the heating (cooling) part of the cycle. A short-circuit current of average magnitude $I = 2P_{sc}A/\tau$ would flow during each cycle, where P_{sc} is the (discontinuous) change in P_s at T_c, and the factor of two arises from the fact that equal but opposite currents are produced during the heating and cooling periods. If a load resistor R is placed in parallel with the sample, it is easily shown [11] that the power dissipated in the load is a maximum for $R = \tau/2\pi\bar{C}$, where $\bar{C}$ is the average value of the sample capacitance during the cycle. If we approximate the current in the load as a square wave and use the relation $\bar{C} = \bar{\epsilon}A/4\pi d$, where $\bar{\epsilon}$ is the average dielectric constant, then we find for the converter efficiency $\eta = I^2R/FA = 2P_{sc}^2/\bar{\epsilon}\Delta Q$. Assuming that the converter is operated in a very small temperature range in the vicinity of T_c, we may identify ΔQ with the latent heat of the phase transition and take for $\bar{\epsilon}$ the average of the limiting

values of ϵ as T_c is approached from above and below.

In the case of $Gd_2(MoO_4)_3$, the material whose behavior suggested this conversion cycle, published values of the dielectric and thermal properties [17] yield an efficiency $\eta = 0.4\%$. Other improper ferroelectrics offer the possibility of higher efficiencies, although their tendency to enter the ferroelectric phase in a single-domain state has not been verified. Iron-iodine boracite ($Fe_3B_7O_{13}I$), for example, yields an efficiency of $\eta \simeq 70\%$ when the data of Schmid et al [19] are used. These results indicate that as investigation continues into the behavior of the boracites and other families of improper ferroelectrics, efforts should be made to determine their usefulness in converters of the type described here.

One final point is worth noting. The conversion cycle proposed above could be used with proper as well as improper ferroelectrics if a means could be found to establish a preferred domain orientation as the material enters the ferroelectric phase. Work on lanthanum doped lead zirconate titanate ceramics [20] has demonstrated that space-charge effects in aged ceramics can establish just such a preference, and this possibility is now under investigation. In the case of a proper ferroelectric with a first-order transition, the efficiency obtained above reduces to $\eta = 8(T_c - T_o)/5\pi T_c$. Using the values tabulated by Jona and Shirane,[21] we find efficiencies for $BaTiO_3$ and $KNbO_3$ of 1% and 4%, respectively. Although these efficiencies must be reduced to account for the fact that the remanent polarization of a ceramic is less than the spontaneous polarization of the corresponding single crystal, they are large enough to suggest

that proper ferroelectrics with strong first-order transitions should be considered for this application.

References

1. S.R. Hoh, Electromech. Design 3, 15 (1959).
2. Electronics, 32-51, 88 (1959).
3. K.H. Spring, Direct Generation of Electricity (Academic Press, 1965) pp. 370-394.
4. W.H. Clingman and R.G. Moore, Jr., J. Appl. Phys. 32, 675 (1961).
5. J.D. Childress, J. Appl. Phys. 33, 1793 (1962).
6. S.R. Hoh, Proc. I.E.E.E. 51, 838 (1963).
7. L. Eyraud, Rev. Gen. Elec. 77, 955 (1968) (In French).
8. J. Perrigot, SC.D. Thesis, Univ. of Lyon, France (1969).
9. C.F. Pulvari and F.J. Garcia, Ferroelectrics 10, 243 (1976).
10. L.J. Sivian, U.S. Patent 2,299,260 (20, Oct. 1942).
11. A. van der Ziel, J. Appl. Phys. 45, 4128 (1974).
12. J.A. Gonzalo, Ferroelectrics 11, 423 (1976).
13. H.M. Choe, J.H. Judy, and A. van der Ziel, Ferroelectrics 15, 181 (1977).
14. A.F. Devonshire, Advan. Phys. 3, 85 (1954).
15. A.P. Levanyuk and D.G. Sannikov, Sov. Phys. JETP 28, 134 (1969).
16. See Appendix C.
17. M.I. Bell, A. Shaulov, Y.H. Tsuo, M. Delfino, G. Loiacono, and W. Smith, Bull. Am. Phys. Soc. 23, 197 (1978).
18. A. Shaulov, private communication.
19. H. Schmid, P. Chan, L.A. Pétermann, F. Teufel, and M. Mändly, Ferroelectrics 13, 351 (1976).
20. K. Okazaki and K. Nagota, J. Am. Ceram. Soc. 56, 82 (1973); K. Okazaki, H. Igarashi, K. Nagota, and A. Hasegawa, Ferroelectrics 7, 153 (1974).
21. F. Jona and G. Shirane, Ferroelectric Crystals (Macmillan, New York 1962) p. 224.

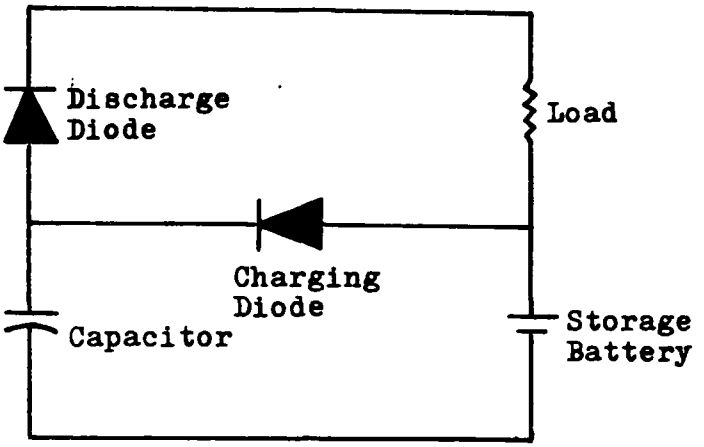

Fig. 1. Typical thermodielectric energy converter circuit.

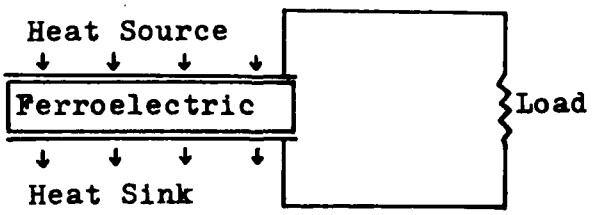

Fig. 2. Typical pyroelectric energy converter circuit.

APPENDIX A

PHYSICAL REVIEW B VOLUME 14, NUMBER 11 1 DECEMBER 1976

Anomalous scattering and asymmetrical line shapes in Raman spectra of orthorhombic $KNbO_3$

A. M. Quittet
Laboratoire de Physique des Solides, Université Paris-Sud, Orsay, France

M. I. Bell
Physics Department, Yeshiva University, New York, New York

M. Krauzman
Département de Recherches Physiques, Laboratoire Associé au Centre National de la Recherche Scientifique No. 71, Université Paris VI, France

P. M. Raccah
Physics Department, Yeshiva University, New York, New York

(Received 27 May 1976)

The Raman spectrum of orthorhombic $KNbO_3$ is found to contain anomalous scattering, consisting of a large background and broad bands, which can be related directly to the dynamic disorder which has been invoked to explain the results of earlier studies of diffuse x-ray scattering and inelastic neutron scattering. Some ordinary first-order lines exhibit coupling to the anomalous part of the spectrum, which is revealed by the existence of resonant interference of the type described by Fano. All these features disappear abruptly at the transition to the low-temperature rhombohedral phase, indicating that they are characteristic of the peculiar dynamics of linear chains observed in the orthorhombic, tetragonal, and cubic phases.

INTRODUCTION

In the ferroelectric perovskites such as $BaTiO_3$ and $KNbO_3$, x-ray diffuse-scattering[1] and inelastic-neutron-scattering[2,3] experiments yield evidence of a very large anisotropy in the dispersion of some of the vibrational modes. Light scattering[1,5] has been used to investigate the zone-center phonons in order to check the soft-mode theories.[6] We report here some new results of Raman scattering experiments performed on a single-domain $KNbO_3$ sample, both in its room-temperature orthorhombic phase and as the temperature is lowered through the orthorhombic-to-rhombohedral phase transition.

The assignment of the ordinary first-order lines is quite easily obtained, leaving outside this classification a large continuous scattering which we refer to as "anomalous." The latter, previously described in Ref. 5 for restricted scattering geometries, has now been found to occur more generally whenever the incident and scattered beams propagate perpendicular to the Z axis and are simultaneously polarized parallel to Z. As expected, this anomalous spectrum disappears abruptly at the orthorhombic-to-rhombohedral transition temperature, as does the normal low-frequency B_2(TO) line. In the spectra where the anomalous scattering occurs, some first-order lines display an asymmetrical shape characteristic of a "Fano interference."[7]

EXPERIMENTAL

The Raman scattering was excited by an argon-ion laser operating at either 4880 or 5145 Å. Measurements were made using a $\frac{1}{4}$-m Spex double-grating spectrometer located at the Maybaum Institute of Yeshiva University and a Coderg T800 triple-grating spectrometer located at Département de Recherches Physiques, Université Paris VI. Both systems employed photon-counting detection.

We used a single-domain sample cut with the faces perpendicular to the orthorhombic axes. Standard right-angle and backscattering geometries were used to obtain various linear momentum transfers from the photons to the crystals. Table I summarizes the modes which can be observed in each scattering geometry. The orthorhombic axes are related to the pseudocubic ones as described in Fig. 1. At zero wave vector, the irreducible representations of the 12 optic modes in the C_{2v} point group of the orthorhombic phase are as follows: $4A_1(X)$, $4B_1(Y)$, $3B_2(Z)$, $1A_2$. All A_1, B_1, and B_2 modes are infrared active (the letters in parentheses indicate the direction of the dipole moment of each mode), and for these the longitudinal or transverse character must be considered. Two features of this table should be noted. First, B_1 and B_2 modes are not detected in a longitudinal configuration. Second, when a polar mode is neither transverse nor longitudinal

TABLE I. Summary of the scattering geometries employed and the mode symmetries observed. Scattering geometries are indicated by the conventional notation $\vec{k}_i(\vec{\epsilon}_i\vec{\epsilon}_s)\vec{k}_s$, where $\vec{k}_i, \vec{\epsilon}_i$ ($\vec{k}_s, \vec{\epsilon}_s$) are the wave vector and polarization vector of the incident (scattered) photon.

				Polarization of incident and scattered beams ($\vec{\epsilon}_i\vec{\epsilon}_s$) and mode symmetry					
	Incident wave vector	Scattered wave vector	Momentum transfer	XX	YY	ZZ	YX,XY	ZX,XZ	(Z,Z)
	$\vec{k}_i$	$\vec{k}_s$	$\vec{k}_s-\vec{k}_i$	A_1	A_1	A_1	B_1	B_2	A_2
Right-angle scattering	X	Y	$\perp Z$	···	···	Mixed	Mixed	TO	Indiff.
	Y	Z	$\perp X$	TO	···	···	Mixed	Mixed	Indiff.
	X	Z	$\perp Y$	···	Mixed	···	TO	Mixed	Indiff.
Backscattering	X	$\bar{X}$	$\parallel X$	···	LO	LO	···	···	Indiff.
	Y	$\bar{Y}$	$\parallel Y$	TO	···	TO	···	···	···
	Z	$\bar{Z}$	$\parallel Z$	TO	TO	···	TO	···	···

in a given scattering geometry (labeled "mixed"), it loses its zero-wave-vector irreducible-representation species through mixing with modes of different symmetry.

ROOM-TEMPERATURE SPECTRA

All the spectra listed in Table I have been recorded. Only those of special interest are reproduced in Figs. 2 and 3. In Fig. 2, the peaks which arise from contamination by other species are drawn with broken lines.

From Table I, and taking into account the possible mixing of species, we can assign the observed frequencies to the different modes. These assignments are summarized in Table II. Within the limit of experimental accuracy, we agree with the results published independently by Winter *et al.*,[5] at least for those lines identified unambiguously in Ref. 5. The following details should be noted. The low-frequency B_2(TO) line (maximum at 40 cm^{-1}) is broad and asymmetrical [Fig. 2(a)], and a thin line at 195 cm^{-1} which sits on its tail is slightly distorted and seems to show a dip on the low-frequency side. In the B_2 mixed spectrum, the lines at 170 and 205 cm^{-1} display an interference dip between them [Fig. 2(b)].

The anomalous spectrum is seen in the following geometries: $Y(ZZ)\bar{Y}$, $X(ZZ)\bar{X}$, and $X(ZZ)Y$. These are A_1(TO), A_1(LO), and A_1(mixed) spectra, respectively, and are shown in Figs. 3(e), 3(a), and 3(c). In each case, the linear momentum transfer is perpendicular to the Z axis, and the light beams are polarized parallel to Z. The anomalous scattering, identical in the three spectra, consists of a continuous background, decreasing in intensity from low to high frequency, and two broad bumps centered near 130 and 430 cm^{-1}.

The ordinary first-order lines are superimposed on the anomalous spectrum, but some of them show a coupling leading to an asymmetrical lineshape and interference dip. This is clearly demonstrated by comparison of the pairs of spectra in Fig. 3:

(i) Figures 3(a) and 3(b): The normal $X(YY)\bar{X}$

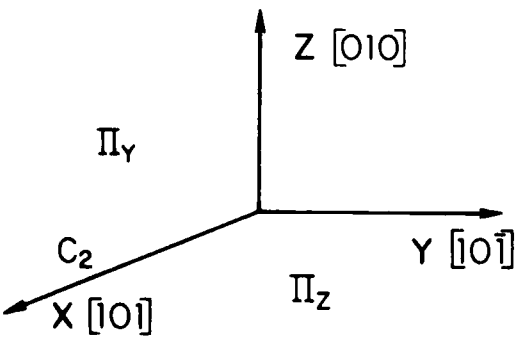

FIG. 1. Orthorhombic axes for $KNbO_3$ and corresponding pseudocubic axes (in brackets). Also shown are the symmetry elements of the C_{2v} point group. The spontaneous polarization is in the X direction.

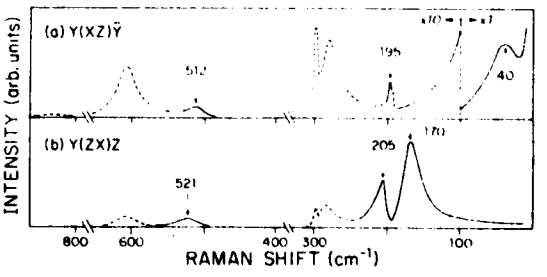

FIG. 2. B_2 symmetry spectra: (a) B_2(TO) in backscattering geometry, (b) B_2 (mixed) in right-angle geometry. The dashed lines indicate contamination from other symmetry species due either to a small misorientation of the polarizers or to mixing of polar modes as described in the text.

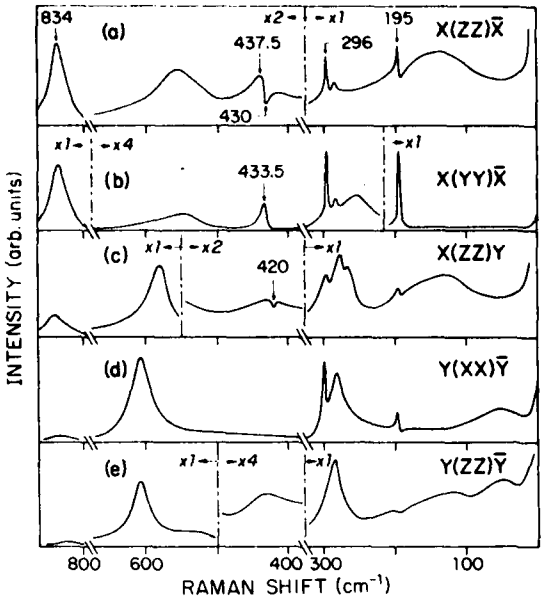

FIG. 3. Anomalous spectra and the associated normal spectra. In the $Y(XX)\bar{Y}$ and $Y(ZZ)\bar{Y}$ spectra, the broad line in the vicinity of 50 cm^{-1} is most probably a contamination from the $Y(XZ)\bar{Y}$ B_2(TO) spectrum due to the divergence of the scattered beam.

spectrum together with the anomalous $X(ZZ)\bar{X}$ one are both A_1(LO) spectra. Note the lines at 195 and 435 cm^{-1}.

(ii) Figures 3(d) and 3(e): The normal $Y(XX)\bar{Y}$ spectrum together with the anomalous $X(ZZ)\bar{Y}$ one are both A_1(TO) spectra. Note the line at 193 cm^{-1}.

(iii) Figure 3(c): The anomalous $X(ZZ)Y$ spectrum has A_1 (mixed) symmetry. Note the mode at

TABLE II. Frequencies and symmetry assignments of first-order Raman lines of $KNbO_3$. The figure in parentheses is the full width of the line at half-maximum.

A_1(TO)	A_1(LO)	B_1(TO)	B_2(TO)	A_2
			40(27×2)	
193(2)	194.5(3)	192(2)	196.5[a]	
		249(25)		
		270		
281.5(33)				282(6)
	295(5)			
297(5)				
	434.5[a](10)			
			513(20)	
		534(20)		
606.5(33)				
	834(27)			

[a] Lines showing an asymmetrical shape in at least one scattering geometry.

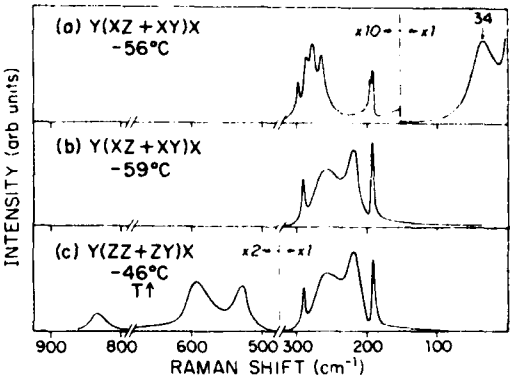

FIG. 4. Temperature dependence of part of the B_1+B_2 spectrum: (a) in the orthorhombic phase just above the phase transition (temperature decreasing), (b) in the rhombohedral phase just below the transition (temperature decreasing), (c) in the rhombohedral phase in the hysteresis interval (temperature increasing).

420 cm^{-1} which appears almost wholly negative in the anomalous part of the spectrum.

TEMPERATURE DEPENDENCE (REF. 8) (23 to −70 °C)

As the temperature is lowered, there is essentially no change in the low-frequency B_2(TO) line and the anomalous spectrum until the transition temperature is reached. The frequency and width of the B_2 line both decrease slightly, but its intensity [Fig. 4(a)], as well as the shape and intensity of the anomalous spectrum, remains unchanged. Below the phase transition, which takes place near −59°C, the spectrum becomes very different [Figs. 4(b) and 4(c)] as the broad B_2 line and the anomalous scattering disappear completely. Since the sample becomes broken and twinned, all the spectra are superimposed, so that it is not possible to miss any lines. Upon reheating the sample, the anomalous spectra of the orthorhombic phase appear again at −30 °C, exhibiting the large thermal hysteresis characteristic of a first-order transition. These experiments thus demonstrate that the anomalous spectrum is related to an intrinsic property of the orthorhombic phase, as is the low-frequency B_2(TO) line.

DISCUSSION

We note first that all the anomalous features which appear in Raman, neutron, and x-ray scattering experiments occur only when the linear momentum transfer lies perpendicular to the Z axis, and that these features disappear in the rhombohedral phase. Hence the dynamical properties of the orthorhombic phase have a pronounced one-dimensional character. These results can be

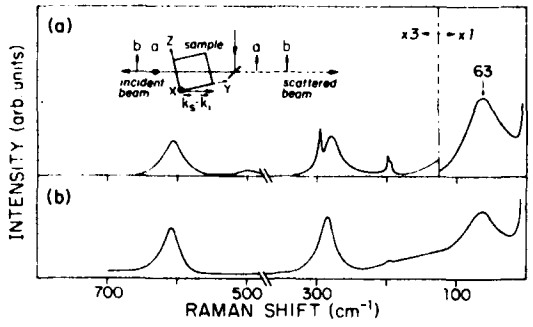

FIG. 5. (a) B_2 spectrum for a momentum transfer rotated by 15° from a TO configuration toward the LO configuration. (b) Anomalous spectrum for the same momentum transfer.

understood[1] as arising from displacements of the niobium atoms in the Z direction (away from the C_2 symmetry axis) which are correlated for some finite distance along Z. Averaged over distances large compared to this correlation length, however, the structure retains orthorhombic symmetry. Such disorder need not be static, since its effects will be seen in scattering experiments provided the lifetime of the local departure from the average symmetry is greater than the scattering time. From this point of view, the anomalous features in the Raman spectra can be interpreted as disorder-induced first-order scattering, i.e., one-phonon scattering by modes which would not be Raman active in a perfect crystal, but which become so when both the translational and point-group symmetries are broken by the disorder. Since all phonons (not only those at the zone center) can become Raman active in this way, one anticipates a scattering spectrum proportional, in first approximation, to the one-phonon density of states. This interpretation is further strengthened by the fact that neutron scattering results[3] suggest the existence of a peak in the one-phonon density of states near 150 cm^{-1}, close to one of the peaks (130 cm^{-1}) in the anomalous Raman spectra.

We have studied the modification of the spectra which occurs as the linear momentum transfer is rotated from the Y direction to the Z direction. As the momentum transfer is changed, the intensity of the anomalous scattering decreases rapidly, while the frequency of the B_2 line shifts very rapidly toward higher values [Figs. 5(a) and 5(b)]. We conclude from this that the B_2 line is produced by an underdamped zone-center phonon with a large LO-TO frequency difference and that the anomalous spectrum in ZZ polarization arises from a continuum of states. Our identification of the line at 40 cm^{-1} as the zone-center B_2(TO) phonon is consistent with the results of neutron scattering experiments.[3] Although Currat *et al.*[3] extrapolate the frequency of the optical branch to about 25 cm^{-1} at the zone center, the experimental resolution is such that spectra near the zone center and at low frequencies are always heavily contaminated by the Bragg peak and the acoustic dispersion. Moreover, the experimental points closest to the zone center could only be obtained from constant-energy scans which do not provide an accurate measure of mode frequency.

The asymmetrical line shapes observed in this work are of two types. One is produced by the small interference between the two lowest-lying lines in the B_2(TO) spectrum [Fig. 2(a)]. This is merely a coupling between modes of identical symmetry, which appears because of the large width of the low-frequency line. The coupling becomes much stronger when the wave vector is rotated 45° from the Y axis toward the Z axis, since the rapid increase in the frequency of the lower mode brings the two modes quite close [Fig. 2(b)].

The second type of asymmetry can be seen in the shape of several narrow lines observed in the anomalous ZZ spectra. This can be analyzed, using a formalism developed by Fano,[7] as an interference between the scattering by a discrete, one-phonon state and a continuum of states. Such line shapes have been reported previously in $BaTiO_3$ by Rousseau and Porto[9] and in heavily doped silicon by Cerdeira *et al.*[10] The application of Fano's formalism to Raman scattering has been treated in detail by Scott.[11] If the Hamiltonian H couples a discrete state φ with a continuum ψ_E according to

$$\begin{aligned} &\langle\varphi|H|\varphi\rangle = E_\varphi\,, \\ &\langle\psi_E|H|\varphi\rangle = V_E\,, \\ &\langle\psi_{E'}|H|\psi_E\rangle = E\delta(E-E')\,, \end{aligned} \tag{1}$$

then the observed scattering cross section σ is related to the cross section σ_E which would be produced by the continuum in the absence of any coupling by

$$\sigma = |(q+\epsilon)^2/(1+\epsilon^2)|\,\sigma_E\,. \tag{2}$$

Here $\epsilon = (E - E_\varphi - \delta E)/\Gamma$ is a reduced energy variable involving the half-width $\Gamma = \pi|V_E|^2$ and energy shift $\delta E = \pi^{-1}\mathrm{P}\int dE'\,\Gamma/(E-E')$ (P indicates "principal part of") of the "resonant" state resulting from the discrete-continuum interaction. The parameter $q = (\pi V_E)^{-1}\langle\Phi|\alpha_{ij}|i\rangle/\langle\psi_E|\alpha_{ij}|i\rangle$ depends on the matrix elements of the Raman tensor α_{ij} for transitions from an initial state $|i\rangle$ to the continuum ψ_E and to the state $\Phi = \varphi + \mathrm{P}\int dE'\,V_{E'}\psi_{E'}/(E-E')$, which is the discrete state φ modified by

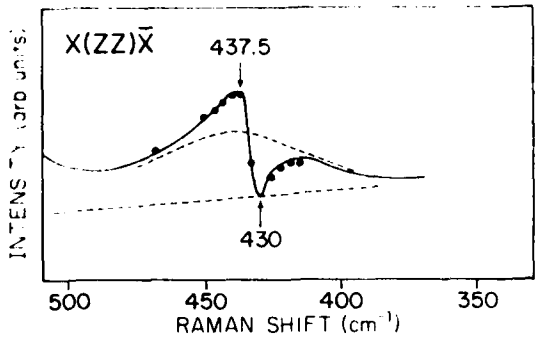

FIG. 6. Comparison of the experimental $X(ZZ)\bar{X}$ spectrum (solid curve) with the prediction of Eq. (2) (dots).

an admixture of continuum states. If q and Γ are independent of E in a sufficiently large interval around E_φ, the spectrum can be fitted to Eq. (2) with q and Γ treated as (energy-independent) fitting parameters. (Note that Γ and q cannot be completely independent of energy unless $\delta E = 0$.) Figure 6 compares the experimental $X(ZZ)\bar{X}$ spectrum near 430 cm^{-1} with the prediction of Eq. (2) to which a slowly varying background has been added. A good fit is obtained for $q = 0.75$, $\Gamma = 3.6$ cm^{-1}, $E_\varphi + \delta E = 432.7$ cm^{-1}. The value of E_φ obtained from the $X(YY)\bar{X}$ spectrum [Fig. 3(b)] is 430 cm^{-1}, yielding a shift $\delta E = 2.7$ cm^{-1} due to the coupling. The exact nature of this coupling remains to be determined. If, as we have proposed, the continuum is produced by disorder-induced first-order scattering, it may be coupled to zone-center modes via anharmonic terms in H as discussed by Scott[11] or via additional terms which depend directly on the disorder.

CONCLUSION

The experiments described here demonstrate that a major part of the dynamical behavior of orthorhombic $KNbO_3$ is one dimensional in character and consistent with the formation of linear chains of correlated displacements of niobium ions as proposed in connection with diffuse x-ray scattering results[1] and Raman scattering studies of the cubic and tetragonal phases.[5] This further evidence of disorder in the orthorhombic phase, together with the observation that the lowest B_2(TO) mode does not display any significant softening with decreasing temperature, strongly suggests that the phase transitions of $KNbO_3$ (including the ferroelectric-paraelectric one) have some order-disorder character. Such a suggestion is not inconsistent with the fact that the transitions are thermodynamically of first order, since recent studies[12] of systems of dipoles interacting via a generalized molecular field have shown that first-order transitions are possible in such a model and that an accurate quantitative description of the cubic-tetragonal transition in $BaTiO_3$ can be obtained.

ACKNOWLEDGMENTS

We are indebted to U. Fluckinger of the Laboratorium für Festkörperphysik, ETH Zurich who provided us with the excellent single-domain $KNbO_3$ sample, to Professor M. Lambert for helpful discussions, and to G. Hamel for technical assistance. The work at Yeshiva University was supported by the Advanced Research Projects Agency.

[1] M. Lambert and R. Comès, Solid State Commun. 7, 305 (1969).
[2] A. C. Nunes, J. D. Axe, and G. Shirane, Ferroelectrics 2, 291 (1971).
[3] R. Currat, R. Comès, B. Dorner, and E. Wiesendanger, J. Phys. C 7, 2521 (1974).
[4] M. P. Fontana and M. Lambert, Solid State Commun. 10, 1 (1972); M. DiDomenico, Jr., S. H. Wemple, S. P. S. Porto, and R. P. Bauman, Phys. Rev. 174, 522 (1968); D. Heiman and S. Ushioda, Phys. Rev. B 9, 2122 (1974).
[5] A. M. Quittet, M. Fontana, M. Lambert, and E. Wiesendanger, Ferroelectrics 8, 585 (1974); F. X. Winter, E. Wiesendanger, and R. Claus, Phys. Status Solidi B 64, 95 (1974).
[6] P. Anderson, in *Proceedings All-Union Conference on the Physics of Dielectrics* (Acad. Sci. USSR, Moscow, 1958), p. 209; W. Cochran, Adv. Phys. 9, 387 (1960) and 10, 401 (1961).
[7] U. Fano, Phys. Rev. 124, 1866 (1961).
[8] Similar results have been reported recently by M. P. Fontana and C. Razzetti [Solid State Commun. 17, 377 (1975)].
[9] D. L. Rousseau and S. P. S. Porto, Phys. Rev. Lett. 20, 1354 (1968).
[10] F. Cerdiera, T. A. Fjeldly, and M. Cardona, Phys. Rev. B 8, 4734 (1973).
[11] J. F. Scott, Phys. Rev. Lett. 24, 1107 (1970); Rev. Mod. Phys. 46, 83 (1974).
[12] M. I. Bell and P. M. Raccah, Bull. Am. Phys. Soc. 20, 349 (1975); Yeshiva University Technical Report No. ECOM-74-0470-1 (1975) (unpublished).

APPENDIX B

Abstract Submitted

for the Washington Meeting of the

American Physical Society

March 1978

Physical Review
Analytic Subject Index
Number 77.80

Bulletin Subject Heading
in which Paper should be placed
Ferroelectrics

Temperature Dependence of the Devonshire Coefficients of Ferroelectrics.* Y.H. TSUO, M.I. BELL, and P.M. RACCAH†, Yeshiva U. - The nonlinear dielectric constants of $BaTiO_3$ and TGS at temperatures above T_c have been measured by means of a large dc bias field and a small audio frequency signal. The coefficient of the term in Devonshire's expression for the free energy which is proportional to the fourth power of the polarization is found to have a strong, linear temperature dependence in both cases. The coefficient of the sixth-power term is also a linear function of temperature in TGS. These results are in qualitative agreement with a recently proposed generalized molecular field theory of ferroelectricity, although certain anomalies which appear in the data for TGS will require further study.

* Supported by ARPA contract DAAB-07-76-C-1342.
† Present address: U. of Ill., Chicago Circle.

APPENDIX C

THEORY OF PYROELECTRIC MATERIALS*

by

M. I. Bell

Abstract

Elementary thermodynamics and simple microscopic models are used to examine the properties of pyroelectric materials which determine their performance as infrared detectors and vidicon targets. It is shown that for small-area detectors the signal-to-noise ratio is subject to a theoretical limit dictated entirely by thermodynamic considerations. In a large class of simple microscopic models for intrinsic (proper) ferroelectrics, the ratio of the pyroelectric coefficient and dielectric constant (which is a figure of merit for vidicon target performance) is found to exhibit an interesting universal behavior. This behavior can be exploited to yield estimates of the figure of merit which suggest that improvements of more than a factor of three are most unlikely using intrinsic ferroelectrics. An examination of extrinsic (improper) ferroelectrics using phenomenological models for the free energy shows that the vidicon figure of merit is not subject to the limitations found for intrinsic ferroelectrics, so that these materials offer the possibility of substantially improved vidicon performance.

* Presented at the July, 1976 meeting of the Defense Advanced Research Projects Agency Materials Research Council.